

## Effects of HVFA with the addition of bottom ash, NaOH, and CaCO<sub>3</sub> on self-compacting concrete (SCC) in tidal environments

Juandra Hartono <sup>a</sup>, Purwanto <sup>b</sup>, Januarti Jaya Ekaputri <sup>a,\*</sup>

<sup>a</sup> Department of Civil Engineering, Faculty of Civil, Planning and Geo Engineering, Institut Teknologi Sepuluh Nopember, Kampus ITS Sukolilo, Surabaya 60111, Indonesia

<sup>b</sup> Department of Civil Engineering, Faculty of Engineering, Diponegoro University, Prof. Soedarto Street, Tembalang, Semarang 50275, Indonesia

### ARTICLE INFO

**Keywords:**

HVFA-SCC  
Fly ash  
Bottom ash  
Tidal zone  
Mechanical properties  
Durability

### ABSTRACT

The study evaluates the impact of exposure to tidal zones over 240 days on the mechanical, microstructural, and durability properties of High Volume Fly Ash - Self Compacting Concrete (HVFA-SCC) for coastal infrastructure applications. The concrete mixture was designed with 60 % and 70 % fly ash (FA) as a replacement for cement, 20 % bottom ash (BA) as a substitute for natural fine aggregate (NFA), 0.05 molar sodium hydroxide (NaOH) as an activator, and 5 % calcium carbonate (CaCO<sub>3</sub>). A comprehensive analysis of workability, flexural strength, displacement, compressive strength, microstructure, chloride ion concentration, and sulfate ion concentration was conducted. The FA content increased, and BA's addition significantly reduced the flow diameter. The combination of NaOH and CaCO<sub>3</sub> successfully modified the rheological properties of the mixture, meeting the SCC criteria. All HVFA-SCC variations demonstrated improved flexural and compressive strengths up to 240 days, while the control mixtures experienced reductions in the flexural capacity of 15.98 % and 14.44 %, respectively. Using FA contributed to a denser microstructure, enhancing durability and flexural toughness. Microstructural analysis shows that HVFA-SCC-70 +BA is more resistant to sulfate attack than the control concrete, characterized by dense C-A-S-H and uniform distribution of elements, despite visible micro-cracks on the surface. The combination of HVFA-SCC-70 +BA with NaOH and CaCO<sub>3</sub> significantly enhances the durability of the concrete in tidal zones, keeping ion concentrations below the threshold level, although it is not as effective as HVFA-SCC-70.

### 1. Introduction

The deterioration of structural capacity in coastal bridges due to corrosion and inadequate concrete design poses a serious global challenge. In Norway, 37 % of 227 prestressed girder bridges in coastal areas exhibit corrosion in their reinforcement [1]. In Shenzhen, China, 85 % of the concrete cover in reinforced concrete bridges shows spalling and cracking due to chloride and sulfate attacks [2]. In Indonesia, the Ministry of Public Works has identified significant damage to drainage systems, girders, decks, embankments, and abutments [3]. Inspections of 35 bridges in the Cirebon-Semarang and Sukabumi-Serang regions reveal a decrease in the capacity of abutments, piers, and girders due to corrosion, with the measured potential of the reinforcement reaching (-0.805 V) against the Ag/Ag+ electrode, along with high resistivity indicating a significant corrosive environment [4].

\* Corresponding author.

E-mail addresses: [juandrahartono@gmail.com](mailto:juandrahartono@gmail.com) (J. Hartono), [purwatrend@lecturer.undip.ac.id](mailto:purwatrend@lecturer.undip.ac.id) (Purwanto), [januarti@ce.its.ac.id](mailto:januarti@ce.its.ac.id) (J.J. Ekaputri).

The intertidal zone (ITZ) is a coastal ecosystem connecting land and sea between the highest and lowest tides. During low tide, this area is exposed to air, while at high tide, it is submerged [5–7]. The zone consists of the supratidal, intertidal (high, mid, and low), and subtidal sections, each characterised by unique features essential for maintaining the balance of coastal ecosystems. Organisms such as barnacles, molluscs, snails, and macroalgae have adapted to withstand wave action, desiccation, and temperature fluctuations. This ecosystem supports a diverse array of marine species and plays a crucial role in nutrient cycling and trophic networks [7–9]. However, marine biodiversity is threatened by various anthropogenic pressures, including pollution from chemical waste disposal, coastal development, and overexploitation, all of which impact ecosystem functionality [10,11]. Therefore, conservation efforts, such as Marine Protected Areas, are essential to protect habitats and biodiversity and emphasize the need for integrated management of tidal ecosystems [12–15].

Extreme conditions in the intertidal zone pose significant challenges to coastal infrastructure, particularly for the concrete structure of the Suramadu Bridge, which is the focus of this study. Located in the Madura Strait and directly connected to the Indian Ocean, the bridge experiences significant sea-level fluctuations: a High Water Level of + 2.445 m, a Low Water Level of –0.005 m, and a Mean Sea Level of + 1.244 m. According to water analysis results, high salt concentrations were detected (37,800 mg/L chloride, 3585.51 mg/L sulfate, and 14 mg/L carbonate), significantly accelerating the corrosion of the steel reinforcement within the concrete. Seawater, following ASTM D1141 [16], contains compounds such as NaCl, MgCl<sub>2</sub>, Na<sub>2</sub>SO<sub>4</sub>, CaCl<sub>2</sub>, KCl, NaHCO<sub>3</sub>, and KBr, with chloride and sulfate ions contributing significantly to the corrosion process, thereby necessitating measures to ensure the concrete's resistance to corrosion. Furthermore, evaluating chloride ingress (ASTM C1202) [17], water absorption (ASTM C642) [18], and sulfate resistance (ASTM C1012) [19] is crucial for understanding the potential damage caused by salts in the intertidal zone.

Various repair methods have been applied to overcome the decrease in structural capacity due to corrosion. This method includes applying jacketing using polymer fiber composite (FRP) materials, High-Performance Fiber Reinforced Cement Composites (HPF RCC), surface treatment, and the application of cathodic protection [20–25]. The goal is to increase the service life of reinforced concrete structures. However, these methods require additional costs, making them less economically efficient [26].

Along with the development of innovations in construction materials, innovative approaches are being explored to improve the durability and service life of concrete structures, especially in coastal areas. These strategies include using concrete with a low water-binding ratio (W/B), replacing some of Portland's cement in concrete with FA [27], [28] or adding nano-sized particles to the concrete mix that result in significant changes to the concrete's microstructure [29]. One innovative concrete developed for this purpose is High Volume Fly Ash - Self-Compacting Concrete (HVFA-SCC), designed with a focus on the long-term durability of structures.

HVFA-SCC is a concrete mix that substitutes at least 50 % of cement weight with fly ash (FA) and exhibits self-compacting properties (SCC) [30–32]. This technology is gaining traction as an environmentally friendly and sustainable alternative to Portland cement-based concrete [33,34], significantly reducing reliance on costly cement, which is a major contributor to CO<sub>2</sub> emissions [35]. The total CO<sub>2</sub> emissions from Ordinary Portland Cement (OPC) reach 84.5 % [36], with the cement industry accounting for 53 % of greenhouse gas emissions in the Industrial Process and Product Use (IPPU) sector [37]. The abundant availability and low cost of FA position HVFA concrete as a viable short-term solution to meet the increasing demand for cement [31]. Meanwhile, SCC offers significant advantages in construction, especially for complex structures. Its high fluidity allows the filling of intricate moulds without mechanical vibration, reducing labour costs and enhancing the final quality of the structure [38,39]. This is particularly beneficial for thin-walled castings and large beams [39–41]. Additionally, SCC accelerates the construction process and minimises defects, resulting in a more consistent and durable end product [31], [42], [43]. However, further research is needed to optimise its applications.

The combination of HVFA and SCC presents significant advantages, especially for large structures in coastal environments. This integration results in concrete with improved volume stability and crack resistance [44,45], as well as lower chloride ion penetration compared to conventional concrete [34,46], thereby protecting reinforcement from corrosion [34,47,48]. Incorporating FA enhances the concrete's resistance to carbonation and chloride diffusion [47] while also improving the workability and flexural strength of SCC [49]. Moreover, FA effectively enhances shrinkage resistance, sulfate resistance, and water absorption [49]. Given its superior mechanical properties and durability, HVFA-SCC holds considerable potential for field applications.

Several studies have explored the influence of FA and other supplementary materials on enhancing the properties of concrete. Filho et al. [50] found that using FA and hydrated lime can reduce calcium hydroxide concentration, improve durability, and decrease chloride ion penetration. Concrete using this combination exhibits a lower chloride diffusion coefficient than High Early Strength Cement (HESC) concrete. Velandia et al. [51] indicated that sodium sulfate could enhance the durability of concrete, particularly with lower chloride penetration in laboratory tests. However, surface treatment increases permeability and carbonation depth. Feng et al. [52] found that combining FA and nano-silica in recycled aggregate concrete can improve mechanical properties, although it may reduce workability. Ribeiro et al. [53] reported that adding fiberglass waste and FA to Portland cement paste increased compressive strength by 32 % and tensile strength by 71 % after 60 days. However, it resulted in a 19 % reduction in density. Maizuar et al. [54] examined the impact of carbon nanotubes (CNT) and graphene oxide (GO) on high-volume fly ash mortars (HVFAM) with 60 % cement replaced by FA. The results showed that adding CNTs and GO reduced working time and accelerated set-up, with an increase in initial compressive strength of 15.8 % and 23 % after 28 days, indicating the potential of environmentally friendly materials.

Golewski [55] examines concrete's physical and mechanical properties with FA for durable composites. The results showed that 30 % FA increased compressive strength and decreased water absorption, while 20 % FA resulted in looser microstructure and increased water absorption. In conclusion, water absorption is inversely proportional to compressive strength. Golewski [56] evaluated the fracture toughness of concrete incorporating a ternary cement blend, utilizing FA and nano-silica (NS). Adding 5 % NS without FA enhanced strength and fracture parameters by approximately 20 %. The combination of 5 % NS with 15 % FA also demonstrated a similar increase, while adding 10 % FA resulted in only a 10 % improvement. This research highlights the potential of FA and NS to reduce the demand for OPC and CO<sub>2</sub> emissions, supporting the development of environmentally friendly concrete.

Furthermore, Golewski [57] conducted a Digital Image Correlation (DIC) analysis, revealing that concrete with nano-silica exhibited straight crack paths, while the combination with FA resulted in curved cracking. Golewski [58] investigated the strength and fracture toughness of concrete composites reinforced with 5 % nano silica (NS) and various contents of FA (0 %, 15 %, and 25 %). The results indicated that adding 5 % NS and FA significantly enhanced the concrete's strength properties and fracture toughness. Concrete containing only NS exhibited delayed fracture processes, while those incorporating NS and FA displayed more complex crack patterns. These findings suggest that NS and FA can improve the performance of concrete for dynamic structures, such as bridges and industrial buildings.

Several similar topics have examined the mechanical characteristics and durability of HVFA-SCC. Meena et al. [59] reviewed the substitution of bottom ash (CBA) and recycled aggregate (RCA) in HVFA-SCC mixtures, finding that 20 % CBA and 25 % RCA significantly increased compressive strength at 120 days. Singh et al. [60] concluded that 20 % CBA substitution improved mechanical behavior and durability, equivalent to SCC control. Singh and Siddique [61,62] recommend optimal CBA substitution of 30 % without and 50 % with superplasticizer. Rafieizonooz et al. [63] found that a 75 % CBA substitution increased flexural strength and tensile strength at 180 days but reduced the work of the concrete. Arjunan et al. [64] studied the activation of alkaline FA in FA-OPC mixture using a low NaOH solution (pH 12.9), which increased the compressive strength of OPC-FA concrete. Fernández-Jiménez et al. [65] found that activating a mixture of 70 % FA and 30 % OPC with NaOH (pH 13.3) resulted in lower potency than water hydration. Pratiwi et al. [66] tested three HVFA PASTE samples and found that a NaOH concentration of 0.03 M was optimal for increasing compressive strength in CN samples [66].

The use of  $\text{CaCO}_3$  in HVFA concrete has a positive effect.  $\text{CaCO}_3$  produces denser microstructures and affects the formation of hydration products, improving the early compressive strength and resistance of HVFA concrete [67]. HVFA concrete with 1 %  $\text{CaCO}_3$  has high compressive strength, low porosity, and high resistance to water absorption, chloride permeability, and chloride ion diffusion [67,68]. Adding FA can slow down the initial hydration and lower the hydration rate of SCC, reducing the initial compressive strength [69]. The presence of  $\text{CaCO}_3$  favours the crystallization of mono carbonates, reacts with tricalcium silicate to form calcium carbo silicate hydrate, and accelerates the development of initial strength [70–72]. The substitution of 50 % cement against FA with 5 %  $\text{CaCO}_3$  has a more progressive compressive strength development than the control FA cement paste [73].

The main challenge in this study is to design HVFA-SCC concrete that meets SCC criteria, such as flowability, passing ability, and segregation resistance [74]. In some cases where HVFA-SCC mixtures use FA substitution for cement exceeding 60 % and BA substitution for fine aggregate exceeding 10 %, the addition of particular chemical additives, in addition to superplasticizers, such as NaOH (sodium hydroxide) and  $\text{CaCO}_3$  (calcium carbonate) becomes crucial for HVFA concrete mixtures to meet SCC criteria. This study uses FA as a partial substitution of cement by 60 % and 70 % and BA as a partial substitution of fine aggregate by 20 %. Using FA is expected to increase concrete's durability and strength, while BA improves the aggregate structure, resulting in more optimal and durable concrete. This study aims to evaluate the effect of FA substitution on cement by 60 % and 70 % and BA substitution on NFA by 20 % with the addition of NaOH chemicals and  $\text{CaCO}_3$ .

The development of existing research shows that investigating the mechanical behavior and durability of HVFA-SCC beams in actual conditions is still very limited because the treatment of test specimens is mainly conducted on a laboratory scale. In addition, the incorporation of FA and BA in HVFA-SCC using chemical additives NaOH and  $\text{CaCO}_3$  has not been extensively investigated. HVFA-SCC research that combines FA substitution of 60 % and 70 % of cement weight and BA substitution of NFA by 20 % has also never been

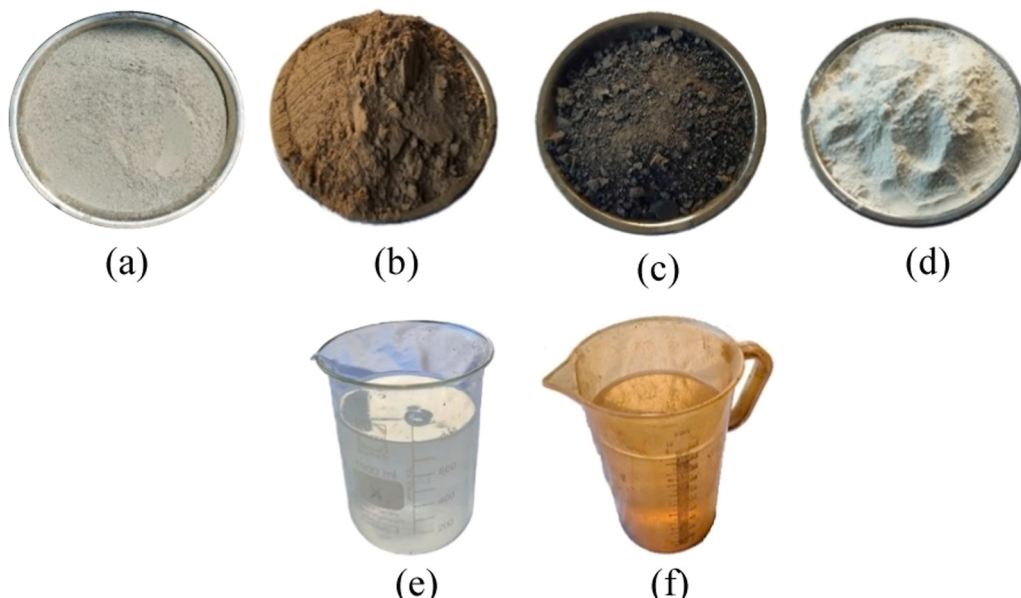


**Fig. 1.** Constituent materials for the formulation of HVFA-SCC (a) OPC cement; (b) fly ash; (c) bottom ash; (d)  $\text{CaCO}_3$ ; (e) NaOH; and (f) water.

conducted. Therefore, further development of the optimal HVFA-SCC mix composition for concrete applications in the marine environment is still an interesting topic to be explored more deeply, considering that the utilization of HVFA-SCC in Indonesia has not been fully realized, especially in large-scale infrastructure projects [75]. The results of this research are expected to contribute to meeting these needs.

## 2. Materials and methods

### 2.1. Materials

The type of cement used is Ordinary Portland Cement (OPC) type 1 based on ASTM C150 standard [76]. The cement was obtained from PT Semen Indonesia (Persero) in Gresik, East Java, Indonesia. Furthermore, FA and BA were obtained from PLTU Paiton Unit 9 in Probolinggo Regency, East Java, Indonesia. Based on the results of the X-ray fluorescence (XRF) test, the FA is included in class F with a CaO (Calcium Oxide) content of 15.75 % according to ASTM C618–19 [77]. The NaOH used is derived from crystals dissolved in clean water with a molarity of 0.05 M, determined through laboratory tests to achieve pH 12, in line with the pH of the cement, to achieve an optimal reaction. In addition, CaCO<sub>3</sub> is used as a filler to replace 5 % NFA. Type F superplasticizer, a water-reducing high-range admixture, is used to improve the workability of concrete following ASTM C494/C494M–05a [78]. Natural fine aggregate (NFA) sourced from Lumajang, East Java, with a particle size of 0.125–4 mm according to SCC criteria [74]. Furthermore, coarse aggregate (CA) in crushed stone came from Pasuruan, East Java, with a maximum size of 20 mm [74]. In the next stage, a trial that includes a mix of design, casting, curing, and testing will be conducted, as illustrated in Fig. 1 and Fig. 2. (Table 1)

### 2.2. Mix design of HVFA-SCC

HVFA-SCC mix planning using ACI 211.4R-08 method [79] and EFNARC methods [74]. There are six variations of HVFA-SCC mixtures, including HVFA-SCC with FA substitution for cement of 60 % and 70 % (HVFA-SCC-60 and HVFA-SCC-70), two variations of HVFA-SCC mixture with FA substitution of 60 % and 70 % and BA substitution for the fine aggregate of 20 % (HVFA-SCC-60 +BA and HVFA-SCC-70 +BA), as well as two variations of HVFA-SCC mixture as control (control-60 and control-70). The detailed proportions of the HVFA-SCC mixture are presented in Table 2. The target compressive strength of the HVFA-SCC at 28 days is set at 50 MPa.

In this study, the variations of HVFA-SCC-70 and HVFA-SCC-70 +BA used NaOH and CaCO<sub>3</sub> additives. The experiment results showed that the mixture's workability was challenging in meeting the SCC criteria if the FA substitution of cement exceeded 60 %, even though a superplasticizer had been added. Therefore, chemical additives are needed that can increase workability with appropriate doses. Chemical additives such as NaOH and CaCO<sub>3</sub> are expected to improve the properties of concrete mixtures to meet the SCC criteria.

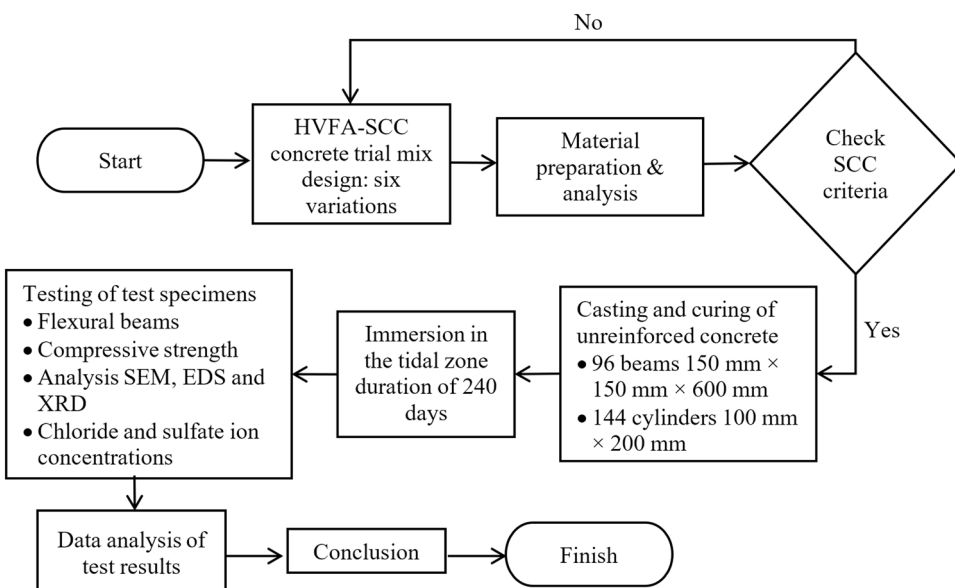


Fig. 2. Flowchart of the HVFA-SCC experiment.

**Table 1**

Chemical analysis of Portland cement, fly ash, and bottom ash (wt%).

Materials	SiO <sub>2</sub>	Al <sub>2</sub> O <sub>3</sub>	Fe <sub>2</sub> O <sub>3</sub>	CaO	MgO	Na <sub>2</sub> O	K <sub>2</sub> O	TiO <sub>2</sub>	MnO <sub>2</sub>	Cr <sub>2</sub> O <sub>3</sub>	P <sub>2</sub> O <sub>5</sub>	SO <sub>3</sub>	LOI
OPC	20.12	5.46	3.35	62.98	1.92	-	-	-	-	-	-	3.62	2.04
FA	37.91	17.85	13.85	15.75	6.54	2.80	1.30	0.69	0.15	0.01	0.33	1.85	0.46
BA	52.70	24.20	8.70	5.20	1.20	1.60	2.40	-	-	-	-	0.70	3.30

**Table 2**

Mix proportions of HVFA-SCC.

Code	Material (kg/m <sup>3</sup> )								
	OPC	FA	BA	Water	Sand	Gravel	Superplasticizer	NaOH 0.05 M	CaCO <sub>3</sub> 5 %
HVFA-SCC-60	194	291		156	883	883	3.87	-	-
HVFA-SCC-60 +BA	194	291	176	156	707	883	3.87	-	-
HVFA-SCC-70	145	339		47	855	879	3.87	109	24
HVFA-SCC-70 +BA	145	339	176	47	679	879	3.87	109	24
Control-60	485	-	-	156	883	883	3.87	-	-
Control-70	485	-	-	156	879	879	3.87	-	-

### 2.3. Specimens: curing and exposure condition

Samples of HVFA-SCC beams measuring 15 cm × 15 cm × 60 cm, as many as 96 pieces, and 144 cylindrical samples measuring 10 cm × 20 cm were printed and left at room temperature for 24 hours. After the beam and cylinder samples have hardened, they are removed from the mould and given a moist curing treatment for 28 days. This process is carried out by covering the entire surface of the test piece using a wet burlap sack and keeping it moist. After passing 28 days, the test specimen is taken to the tidal zone for immersion for 1–8 months. The immersion of the test piece is located just below the Suramadu bridge area on the Surabaya side, East Java, Indonesia, on pillar number 1 between pillars 5–6, 6–7, 7–8, and 8–9. A field review and the results of seawater quality tests inform the selection of this location. The analysis of the water samples and the immersion site within the tidal zone is presented in Table 3 and Fig. 3.

### 2.4. Testing of the specimens

This study evaluated the properties of HVFA-SCC concrete specimens, focusing on strength and durability characteristics. The type of test includes an assessment of workability based on SCC acceptance criteria, bending capacity, ductility, and compressive strength. In addition, advanced analysis was carried out using Scanning Electron Microscopy (SEM), Energy Dispersive X-ray Spectroscopy (EDS), and X-ray Diffraction (XRD). Measurements of chloride and sulfate ion concentrations were also included in this study. The entire test is conducted to provide a comprehensive understanding of HVFA-SCC concrete performance, covering aspects ranging from flowability to stability and reliability.

#### 2.4.1. Workability

The ability to flow fresh concrete will be tested according to SCC criteria: Slump Flow, L-box, and V-funnel testing. The EFNARC 2005 standard establishes a slump flow value limit between 650 mm to 800 mm. The higher the Slump Flow (SF) value, the better the ability to fill gaps in the formwork or mould. For L-box testing, the limit (H<sub>2</sub>/H<sub>1</sub>) is between 0.8 and 1.0. The higher the blocking ratio value, the easier the concrete to flow. Meanwhile, the V-funnel flow limit is 6–12 seconds [74]. If the concrete flow is intermittent, the test must be repeated. If this condition occurs twice or more, the concrete is considered too thick and cannot be categorized as SCC. Details of SCC test results can be seen in Table 4.

#### 2.4.2. Flexural capacity

The flexural strength test method on HVFA-SCC mixtures uses simple beams with the *Third Point Loading approach*, following ASTM

**Table 3**

Analysis of seawater quality in the Suramadu Bridge area.

Parameters	Unit	Analysis results	Analysis methods
Free Chloride	Mg/L Cl <sup>-</sup>	18,600.00	Argentometri
Chloride bonded	Mg/L Cl <sup>-</sup>	19,000.00	Argentometri
Sulfate-free	Mg/L SO <sub>4</sub>	1132.06	Spektrofotometri
Sulphate bound	Mg/L SO <sub>4</sub>	2322.33	Spektrofotometri
Carbonate (Ca <sub>CO<sub>3</sub></sub> )	Mg/L Ca <sub>CO<sub>3</sub></sub>	14.00	Aside-Alkalimetri
Bicarbonate	Mg/L Ca <sub>CO<sub>3</sub></sub>	63.00	Aside-Alkalimetri

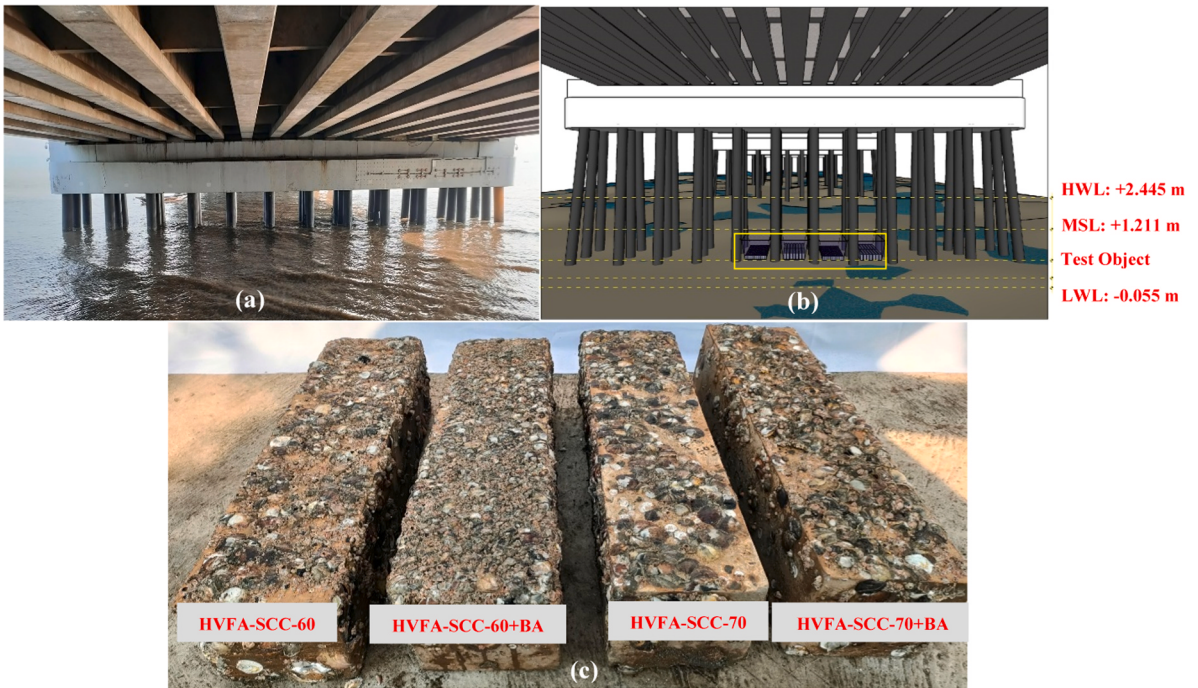


**Fig. 3.** Location of immersion of test objects in the tidal zone, Suramadu Bridge (a) high tide; (b) placement of test specimens; and (c) HVFA-SCC beam sample 240-days immersion.

**Table 4**  
Workability of HVFA-SCC.

Type of testing	Testing standards		HVFA-SCC mix variation					
	Min	Max	HVFA-SCC-60	HVFA-SCC-60 +BA	HVFA-SCC-70	HVFA-SCC-70 +BA	Control-60	Control-70
Slump flow (mm)	650	800	678	670	668	662	685	680
V-funnel (sec)	6	12	10	10	11	12	10	11
L-box ( $h_2/h_1$ )	0.8	1.0	0.9	0.9	1.0	1.0	0.9	1.0

C-78 standard [80]. Flexural strength testing was carried out on a beam sample measuring 150 × 150 × 600 mm after immersion in the tidal zone for 1–8 months. The test procedure is performed by placing the test piece on two platforms, where a centralized load is applied in the middle of the span. The loading is carried out continuously to avoid shock effects affecting the test results. The test settings and bending beam test results can be seen in Figs. 4 and 5.

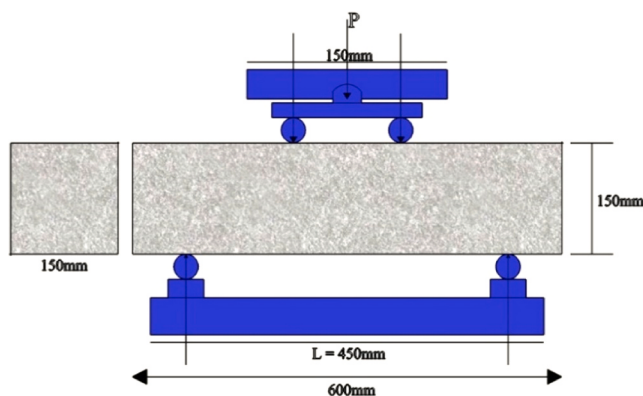


**Fig. 4.** Bending beam geometry.

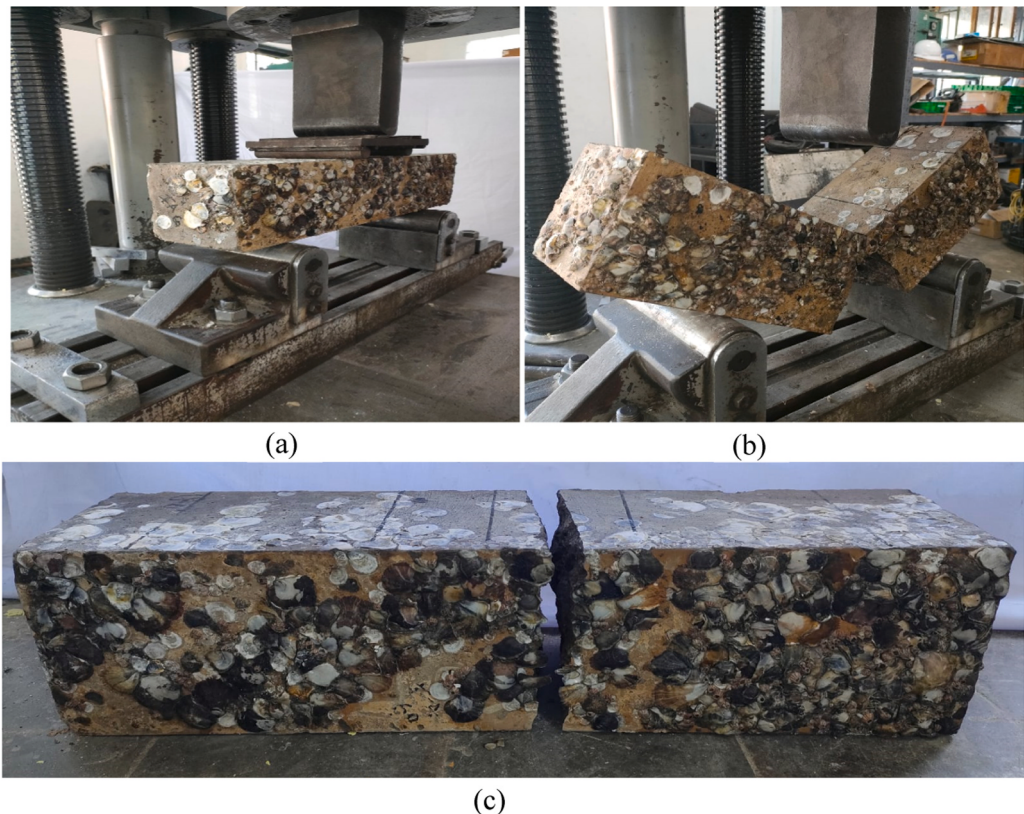


**Fig. 5.** HVFA-SCC-60 beam immersion duration at 240 days: (a) HVFA-SCC-60 concrete specimen during flexural testing, (b) Specimen failure post-test, (c) Crack pattern of HVFA-SCC-60 beam.

#### 2.4.3. Deflection

The load is applied gradually using a compression testing machine until the HVFA-SCC beam reaches the point of failure. During this process, deflection and strain measurements are performed continuously. The test is continued until the beam cracks or fails to observe the relationship between the load and deflection. After the test, the data obtained is analyzed to get the maximum deflection value of the HVFA-SCC beam. This analysis compares the maximum load received and the deflection that occurs.

#### 2.4.4. Compressive strength

All variations of HVFA-SCC are tested for compressive strength following ASTM C39/C39M-18 ASTM C39/C39M-18 standards [81]. Compressive strength testing was carried out on a cylinder sample measuring 100 mm × 200 mm after immersion in the tidal zone of seawater for 1, 2, 3, 4, 5, 6, 7, and 8 months. This compressive strength test aims to evaluate the mechanical performance of HVFA-SCC mixtures under extreme environmental conditions. The outcomes of this test are anticipated to yield valuable insights into the durability and stability of HVFA-SCC in structural applications.

#### 2.4.5. Microstructural analysis

The methodology of Scanning Electron Microscopy (SEM) is employed to evaluate the microstructural attributes and morphological characteristics of HVFA-SCC specimens. SEM analysis utilizes a scanning electron microscope to acquire high-resolution images. In this study, Energy Dispersive Spectroscopy (EDS) is conducted concurrently with SEM imaging to ascertain the elemental composition of the HVFA-SCC formulation. The specimens undergo SEM and EDS analysis following immersion in the tidal zone for six months. The findings of this investigation are anticipated to provide profound insights into the effects of environmental conditions on the microstructural features of HVFA-SCC. X-ray Diffraction (XRD) analysis aims to comprehensively identify the mineral phases and microstructural changes occurring in HVFA-SCC after a specified immersion period in tidal environments. This testing is crucial for understanding the mineral transformations that influence the mechanical properties of the concrete.

#### 2.4.6. Concentration of chloride and sulfate ions

Testing the concentration of chloride ions in concrete is carried out by argentometry titration to determine chloride levels. This method follows ASTM C1556 [82] and (ASTM C1202) standards. In addition, sulfate concentrations in concrete can be measured using spectrophotometry following the ASTM C114-09 standard [83] and (ASTM C1012) [19], which helps evaluate the risk of sulfate damage. In this study, the 240-day-old test samples immersed in the tidal zone were tested at 0 mm and 25 mm depths, representing

the concrete's surface and inner layers. Afterwards, the samples were crushed and filtered using sieve number 200 for further analysis. This method provides an understanding of the distribution of ions in concrete and its impact on the strength of the material.

### 3. Analysis and discussion

#### 3.1. Workability of HVFA-SCC

HVFA-SCC fresh concrete mix workability tests include slump flow, V-funnel, and L-box tests outlined in [Table 4](#). The results indicate that the HVFA-SCC-60 variation provides the best workability compared to other HVFA-SCC mixtures. Adding BA by 20 % to the HVFA-SCC-60 +BA variation reduces workability compared to mixtures without BA. The spherical characteristics of FA particles serve as microbeads, which improve the flow ability of SCC concrete [84–86]. However, when FA and BA are mixed, the morphological difference between the two increases the shear friction in the binding paste, which impacts decreasing the slump flow value of the mixture [87,88]. This phenomenon underscores the importance of the composition and physical properties of the aggregate in influencing the workability of concrete mixtures.

Similar occurrences can be seen in HVFA-SCC-70 and HVFA-SCC-70 +BA mixtures. Although both variations meet EFNARC standards, their slump flow values are still lower than HVFA-SCC-60 and HVFA-SCC-60 +BA. An increase in FA substitution above 60 % and adding BA led to a decrease in flow diameter, with a decline of 1.47 % and 1.65 %, respectively, compared to HVFA-SCC-60 and HVFA-SCC-60 +BA. This decline is influenced by several factors related to the materials' properties. Higher FA content tends to increase viscosity, which can inhibit the flow ability of the mixture. Research shows FA concentrations above 60 % can potentially increase porosity and reduce homogeneity, negatively impacting flow characteristics [89].

Meanwhile, adding BA, while beneficial in specific contexts, can exacerbate the decrease in flow diameter when combined with high levels of FA. The combination of the two creates more complex rheological behaviors, resulting in a reduction of mixed flowability [90]. Overall, the test results showed that the slump flow values for HVFA-SCC-60, HVFA-SCC-60 +BA, HVFA-SCC-70, and HVFA-SCC-70 +BA mixtures were lower than those of the controls, with percentage decreases of 1.02 %, 2.19 %, 1.76 %, and 2.19 %, respectively.

HVFA-SCC concrete mixtures containing BA, NaOH, and CaCO<sub>3</sub>, such as HVFA-SCC-70 +BA, exhibit lower workability than HVFA-SCC-70 without BA. Nevertheless, the slump flow values of the two mixtures still meet the acceptance criteria. The addition of NaOH functions to increase FA reactivity accelerates the formation of C-S-H (Calcium-Silicate-Hydrate) gel, which acts as a lubricant, reduces friction between particles, and increases the fluidity of concrete [91,92]. In addition, the presence of CaCO<sub>3</sub> seems to favor the crystallization of monocarbonates rather than monosulfates. CaCO<sub>3</sub> reacts with tricalcium silicate to form calcium carboaluminate hydrate, which has a significant effect on the cement hydration process and the simultaneous FA pozzolanic reaction [70,71], [93]. If CaCO<sub>3</sub> accelerates the hydration of the cement and the FA reaction, then the water requirement in the concrete mixture can be reduced, improving the mix's performance ability. The indirect effect of CaCO<sub>3</sub> on workability can occur through a reduction in water requirements, depending on the amount of CaCO<sub>3</sub> used.

L-Box and V-Funnel tests were carried out to evaluate the filling capabilities of HVFA-SCC concrete. The test results showed that all HVFA-SCC mixtures met EFNARC standards regarding filling ability and viscosity. The L-Box test's ratio (h<sub>2</sub>/h<sub>1</sub>) ranged from 0.8 to 1.0, while the flow time on the V-Funnel ranged from 6–12 seconds. NaOH plays an essential role in controlling the viscosity

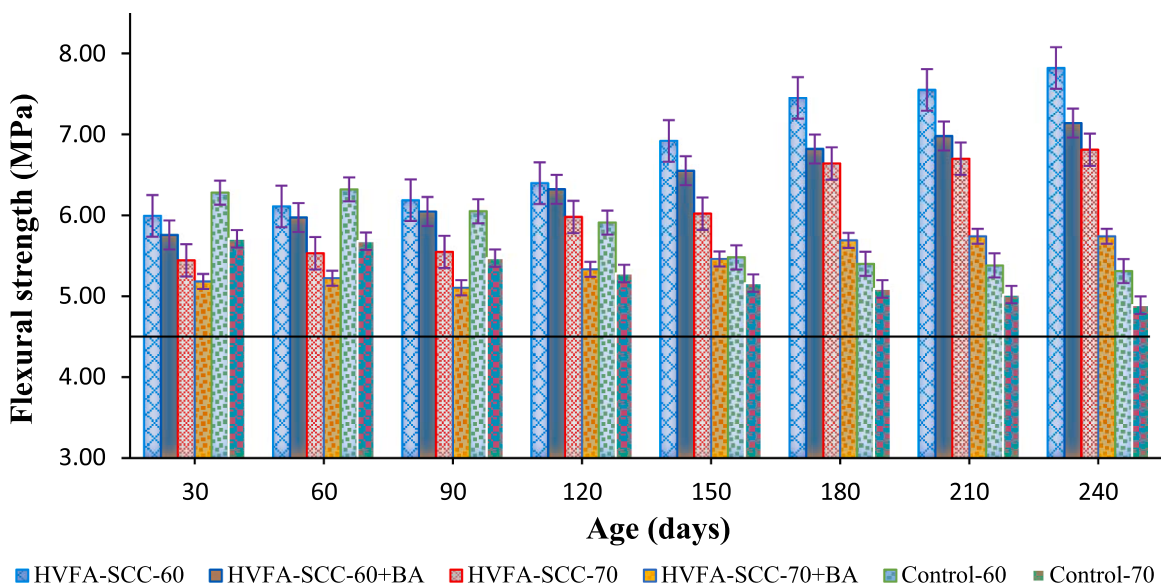


**Fig. 6.** Flexural capacity of HVFA-SCC beams.

of concrete. Excessive viscosity can inhibit the flow and compaction of concrete. Adding NaOH helps reduce viscosity by increasing the formation of C-S-H gel, a lubricant [94].

### 3.2. Flexural capacity

After being subjected to immersion conditions in the tidal zone of seawater, the bending capacity of HVFA-SCC beams is significantly different from that of the control. Fig. 6 shows the bending capacity of HVFA-SCC beams with FA substitution to cement of 60 % and 70 %. Over a 30–240-day immersion period, HVFA-SCC beams showed a consistent increase in bending capacity, with HVFA-SCC-60 achieving the highest bending capacity of approximately 7.82 MPa at 240 days of age, followed by HVFA-SCC-60 +BA (7.14 MPa), HVFA-SCC-70 (6.81 MPa), and HVFA-SCC-70 +BA (5.74 MPa). In contrast, the control-60 variation decreased by 15.98 % in the 90–240-day age range, which showed a significant downward trend. On the other hand, control-70 experienced a decrease of 14.44 % in the age range of 60–240 days.

This finding shows that HVFA concrete has comparable or even better performance and mechanical durability than traditional concrete, especially in marine environments [95]. Raheel et al. [96] reported a substantial increase in flexural capacity in HVFA concrete, with a figure of 57 % at 120 days of age. The use of FA contributes to the formation of denser microstructures by filling pores and reducing pore spacing, thereby increasing the strength and durability of resistant concrete [96,97]. The findings presented by Wang et al. [98] suggest that the physical and mechanical characteristics of concrete structures utilized in marine environments, along with hydraulic concrete exposed to fluctuations in tidal conditions and groundwater levels, undergo significant deterioration due to alternating dry and wet cycles, as well as sulfate assaults. Adding FA can increase the resistance of concrete to sulfate attack in wet-dry cyclic conditions. In addition, long-term loads can worsen chloride penetration in the compressive and tensile areas of concrete structures [99].

Incorporating 20 % BA as a substitute for NFA significantly enhanced the flexural strength of HVFA-SCC-60 +BA and HVFA-SCC-70 +BA beams over an immersion period of 240 days. However, this improvement was still inferior to that observed in the HVFA-SCC-60 and HVFA-SCC-70 configurations. These findings corroborate the research by Meena et al. [59], which explored the utilization of BA and recycled concrete aggregate (RCA) as partial replacements for NFA and natural coarse aggregates (NCA) in HVFA-SCC formulations. The study assessed variations in BA and RCA proportions ranging from 0 % to 30 % and 0–50 %, respectively. Experimental results indicated that combining CBA (20 %) and RCA (25 %) in HVFA-SCC substantially increased the concrete's flexural and shear strength at the 120-day mark. Furthermore, research by Singh et al. [60] demonstrated that substituting NFA with BA in optimal proportions (up to 20 %) yielded enhanced mechanical properties and durability of SCC concrete.

In addition, adding NaOH and CaCO<sub>3</sub> has significantly impacted the bending strength of HVFA-SCC beams. Research shows that NaOH functions as an alkaline activator, accelerating the process of developing the strength of concrete in the marine environment [100]. Meanwhile, adding CaCO<sub>3</sub> contributes to microstructural improvements, increasing strength [101]. These findings emphasize the importance of using alternative materials to develop more potent and durable concrete materials.

### 3.3. Displacement

The flexural testing of the HVFA-SCC beam without reinforcement is conducted to evaluate the resulting deflection. In Figs. 7 and 8,

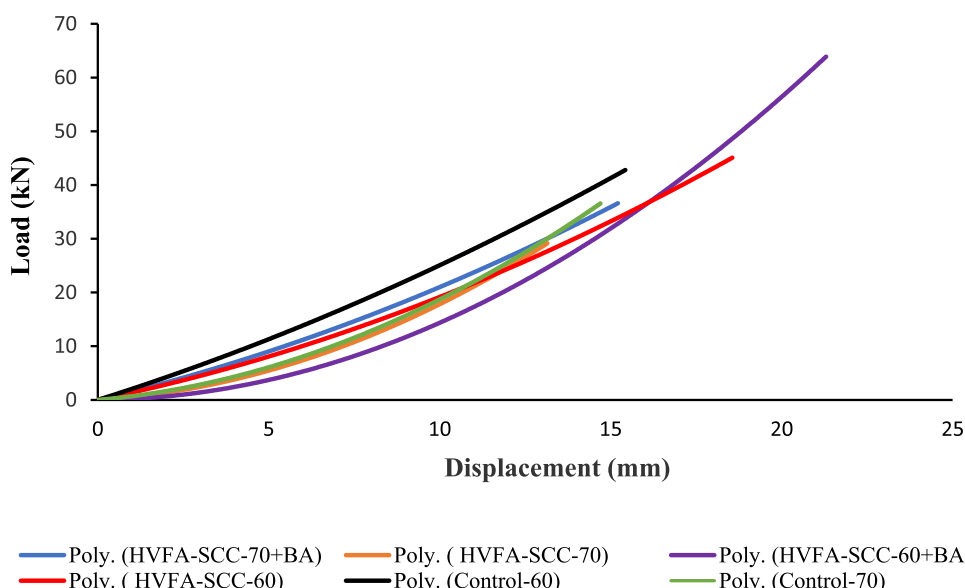


Fig. 7. Deflection of HVFA-SCC beam at 28 days.

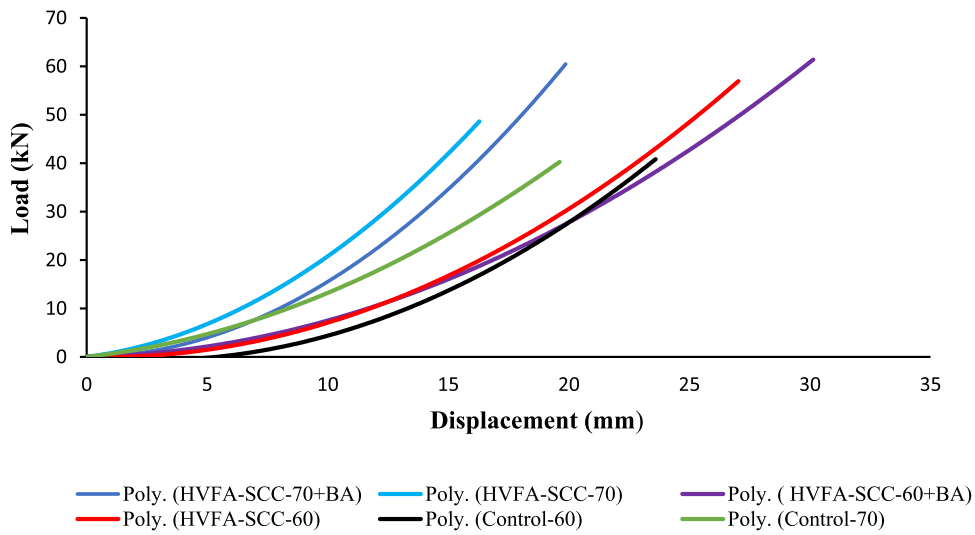


Fig. 8. Deflection of HVFA-SCC beam at 240 days.

the relationship between the load and deflection of the HVFA-SCC beam without reinforcement is shown through bending testing. Fig. 7 shows the results of the bending strength test of the beam at the age of 28 days. Each beam variation experiences an increase in deflection as the load increases, with the HVFA-SCC-60 and HVFA-SCC-60 +BA beams reaching the highest maximum loads of 46.84 kN and 54.50 kN, respectively, with a deflection of 18.56 mm and 21.3 mm.

Meanwhile, the HVFA-SCC-70 and HVFA-SCC-70 +BA beams can only withstand maximum loads of 33.55 kN and 40.20 kN, with a deflection of 13.15 mm and 15.21 mm, respectively. Compared to the control beam, the HVFA-SCC-60 and HVFA-SCC-60 +BA variations exhibit a higher maximum load and deflection than the control beam-60. In contrast, the HVFA-SCC-70 variation results in a maximum load and lower deflection than the control beam-70. However, the HVFA-SCC-70 +BA beam performs better than the control beam-70.

Fig. 8 shows the relationship between load and deflection on HVFA-SCC beams and control beams immersed in the tidal zone of seawater for 240 days. The pattern looked similar to the test at 28 days of age, where the HVFA-SCC-60 +BA variation recorded the maximum load and the highest deflection, followed by the HVFA-SCC-60 and the control beam-60, with values of 67.57 kN, 59.39 kN, and 48.22 kN, respectively, and a deflection of 30.13 mm, 27.03 mm, and 23.60 mm. Interestingly, the HVFA-SCC-70 variation significantly improves, with a better maximum load and deflection than the control beam-70. However, the results are still lower than HVFA-SCC-70 +BA.

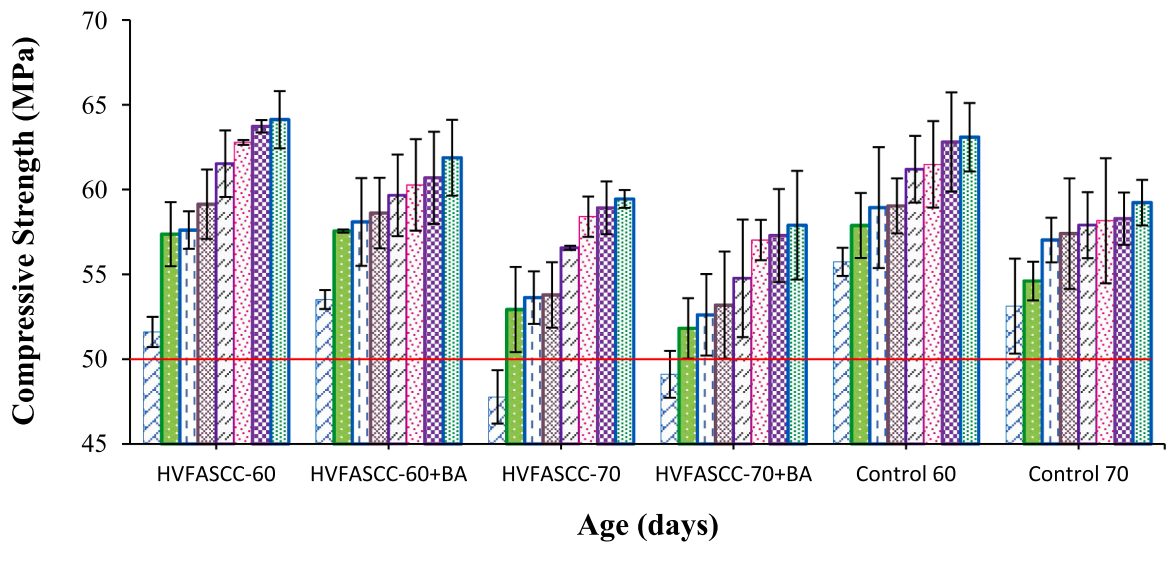


Fig. 9. Compressive strength of HVFA-SCC concrete.

The findings indicate that incorporating FA as a substitute for cement and BA as fine aggregate in HVFA-SCC can enhance structural performance, particularly under extreme conditions. Adding FA up to a certain limit can reduce deformation in beams. Research by Jin et al. [102] supports this result, showing that deflection in reinforced HVFA-SCC beams increases with higher FA content, especially at 90 days of age. Furthermore, adding FA positively affects the flexural toughness of beams; however, after reaching a certain ratio, further increases in FA content do not significantly enhance the material's flexibility. The recommended FA ratio of 76 %, as suggested by Jin et al. [102] as optimal for structural applications, refers to the proportion of FA to the total binder materials (cement + FA) derived from the FA3.2 mix (1 kg of cement, 3.2 kg of FA), which demonstrates improved mechanical performance (double cracking, strain hardening, compressive strength exceeding 30 MPa at 28 days). Additional findings presented by Liu et al. [39] indicate that adding steel fibers significantly enhances the mechanical properties of fracture in high-volume fly ash self-compacting concrete (HFSCC) with varying percentages of FA. Analysis reveals that the relationship between peak load ( $F_p$ ) and deflection in SCC with high-volume fly ash (HFSCC) increases linearly with rising FA content, peaking at 70 % FA. Moreover, GF HFSCC with a uniform volume fraction of steel fibers ( $V_f$ ) also shows improvement, indicating better resistance to crack propagation. SEM tests confirm that at 70 % FA, the pozzolanic reaction is more effective, producing hydration products that fill voids and strengthen the concrete matrix. Consequently, the maximum peak load and deflection values are achieved at 70 % FA, where the concrete matrix attains optimal density and strength. The composition of HFSCC-70 consists of cement (141.5 kg), FA (275 kg), quicklime (62.5 kg), water (170 kg), sand (833 kg), gravel (833 kg), and water reducer (0.91 kg), collectively yielding optimal mechanical performance. Fajrul et al. [103]. The reported results are different from those of the control beam. The analysis indicates that HVFA-SCC beams have better stress-hardening properties, likely contributing to lower deflection values.

### 3.4. Compressive strength

The compressive strength test results of HVFA-SCC concrete treated in the tidal zone of seawater for 30–240 days, as shown in Fig. 9, demonstrate a significant increase in compressive strength for both HVFA-SCC concrete and the control up to a 240-day immersion period. After 30 days, the HVFA-SCC-60 and HVFA-SCC-60 +BA variations achieved strengths exceeding the planned target of 50 MPa, with respective increases of 3.19 % and 7.03 %. After 240 days of immersion in tidal zones, the compressive strength testing confirms the long-term advantages of HVFA-SCC concrete. The compressive strength of HVFA-SCC, particularly in the variations with 60 % and 70 % fly ash substitution, demonstrates a significant improvement compared to the control concrete. HVFA-SCC-60 achieved a compressive strength of 64.12 MPa, while HVFA-SCC-70 reached 59.44 MPa. In contrast, the control mixes with 60 % and 70 % substitution only attained strengths of 63.09 MPa and 59.23 MPa, respectively.

A different outcome was observed for the HVFA-SCC-70 and HVFA-SCC-70 +BA variations; after the 30-day immersion period, neither achieved the target compressive strength outlined in the plan. In line with these findings, Jiang et al. [101] research suggests that FA contributes positively to strength development, but its effectiveness may decrease at higher replacement rates. These findings indicate a threshold at which the strength of concrete begins to decline. When the proportion of FA in HVFA concrete exceeds 60–70 %, the mechanical properties, especially the compressive strength at an early age, tend to decrease [35]. FA is a pozzolanic material that reacts with calcium hydroxide  $\text{Ca(OH)}_2$  during cement hydration, producing calcium silicate hydrate (C-S-H) as an essential binder. However, if the proportion of FA is too high, the hydration reaction can be inhibited, reducing the amount of C-S-H formed [104].

After 180 days of immersion in tidal zones, HVFA-SCC-70 achieved a compressive strength of 58.40 MPa, slightly surpassing Control-70, which recorded 58.16 MPa. At the 240-day measurement, HVFA-SCC-70 rose to 59.44 MPa, while Control-70 reached 59.23 MPa. HVFA-SCC-70 +BA also exceeded the 50 MPa target at 60 days, attaining 57.90 MPa after 240 days, indicating a consistent upward trend. These findings support the research of He et al., who stated that HVFA concrete can significantly increase compressive strength and durability, especially in seawater environmental conditions, with an increase of 13.22 % [105]. In addition, HVFA concrete generally exhibits mechanical performance and durability that is equal to or even better than concrete without FA, as evidenced in previous studies [32], [95], [106]. In addition, the graph demonstrates that the compressive strength of HVFA-SCC mixtures incorporating Bottom Ash (BA) is slightly lower than those without BA during the 120–240-day period. However, all mixtures successfully maintained strength levels above the 50 MPa threshold.

Several interrelated factors can explain the decreased compressive strength in mixtures containing BA differences in particle size, pozzolanic activity, and water absorption characteristics [107,108]. BA's relatively larger and less uniform particle size significantly reduces the pozzolanic reaction surface area. FA, with finer particles and a more uniform size distribution, offers a greater surface area, facilitating more efficient reactions with calcium hydroxide  $\text{Ca(OH)}_2$  to produce calcium silicate hydrate (C-S-H) [109]. C-S-H is the primary hydration product responsible for the strength and durability of cementitious materials. Therefore, BA's larger particle size inherently limits the pozzolanic reaction rate, resulting in less C-S-H formation and, consequently, lower compressive strength [108].

Additionally, the lower pozzolanic activity of BA compared to FA further contributes to the reduction in compressive strength [110]. FA typically contains higher levels of amorphous silica and alumina, the active components in pozzolanic reactions. This amorphous structure is more reactive than the crystalline phases present in BA, which tend to be less reactive. As a result, FA demonstrates a greater capacity to react with  $\text{Ca(OH)}_2$  and produce C-S-H, thereby enhancing the strength and density of the cement matrix [111].

Furthermore, the water absorption characteristics of BA play a crucial role in influencing compressive strength. BA generally exhibits higher internal porosity and a rougher surface structure, leading to increased water absorption. Excessive water absorption can disrupt cement's hydration process, resulting in larger and more interconnected pores within the cement matrix [112]. This increased porosity weakens the material's internal structure, reducing its compressive strength. Additionally, water trapped in the pores may undergo freeze-thaw cycles in harsh environments, causing further damage and reducing the material's durability.

The amalgamation of 70 % FA, 20 % BA, 0.05 M NaOH, and 5 % CaCO<sub>3</sub> in the HVFA-SCC-70 +BA variant has been demonstrated to enhance the compressive strength of concrete at later ages; however, the outcomes remained inferior to those of the HVFA-SCC-60, HVFA-SCC-60 +BA, and HVFA-SCC-70 variants. Incorporating CaCO<sub>3</sub> yields calcium that engages in a pozzolanic reaction with the silica and alumina present in FA, thereby promoting the generation of supplementary calcium silicate hydrate (C-S-H), critical for strength development [113]. Concurrently, NaOH amplifies the reactivity of FA and expedites the synthesis of C-S-H, which functions as the principal binding agent in concrete. These findings indicate that the combination of additives may contribute to improved mechanical performance of concrete, especially in applications that require high durability.

### 3.5. Microstructure analysis

#### 3.5.1. SEM (Scanning electron microscopy) and EDS (Energy dispersive X-ray spectroscopy)

An analysis of the microstructure of HVFA-SCC-70 +BA concrete immersed in a tidal area of seawater for 180 days is shown in Fig. 10, which presents the test results using Scanning Electron Microscope (SEM) and Energy Dispersive X-ray Spectroscopy (EDS) to understand its morphological properties. Fig. 9(a) shows the microstructure of the HVFA-SCC-70 +BA Outer Code with 1000x magnification. A dominant C-A-S-H matrix indicates good hydration from FA and BA. The spherical and evenly distributed FA particles are visible, indicating a positive contribution to the density of the concrete. From the observation results, it is also seen that some FA have not reacted. Exposure to marine environments containing aggressive ions can affect hydration processes and pozzolanic reactions, thus inhibiting FA reactions. Although it has been soaked for six months, that time may not be enough to ensure all FA reacts. Another reason may be related to the physical and chemical properties of the FA used [114].

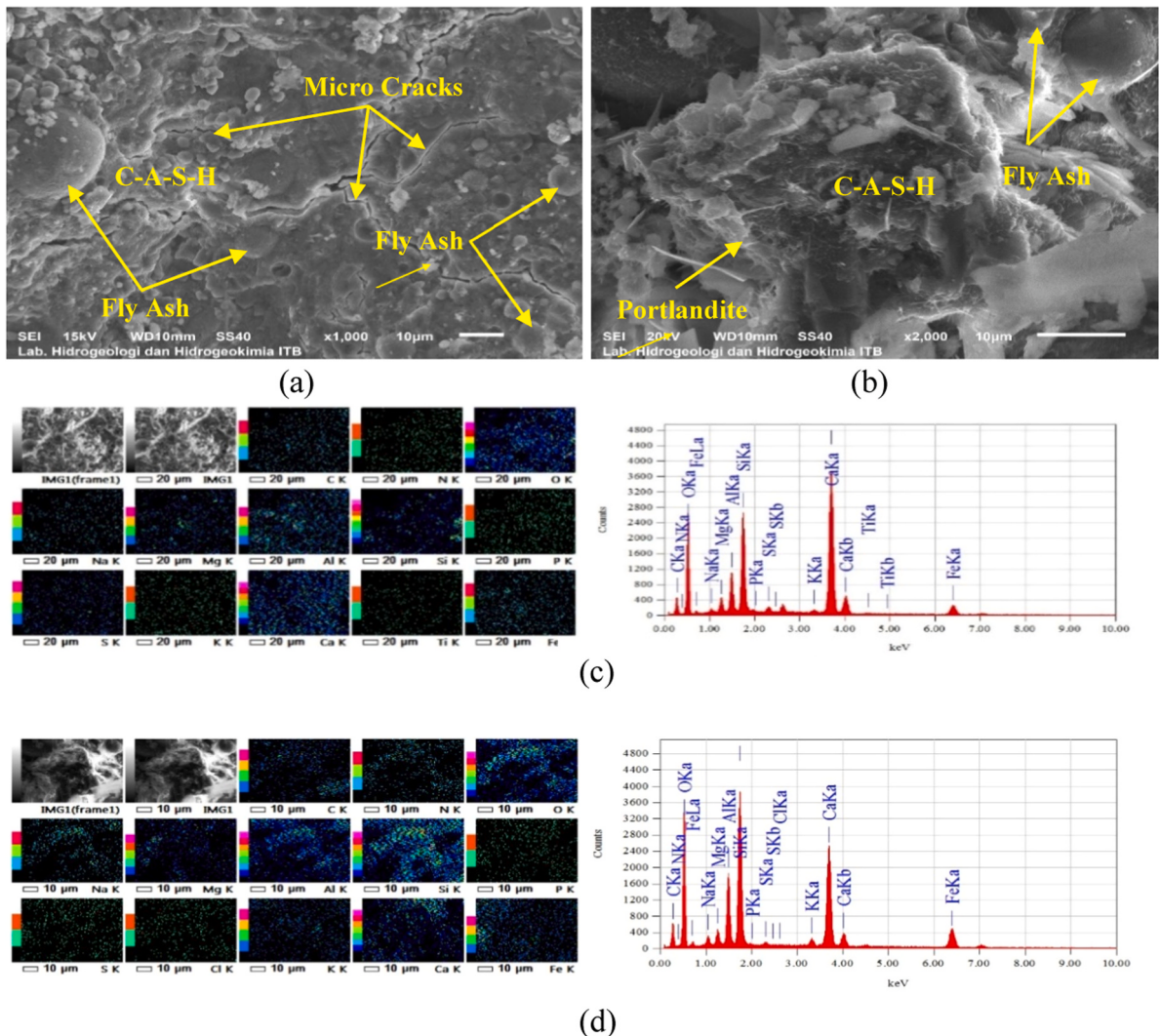


**Fig. 10.** SEM and EDS images of HVFA-SCC-70 +BA at 180 days of immersion: (a and c) HVFA-SCC-70 +BA Outer Code, (b and d) HVFA-SCC-70 +BA Inner Code.

Microcracks indicate potential susceptibility to damage, which may be caused by shrinkage or external pressure during a 180-day immersion period. Porous BA particles can cause uneven distribution of water in the mixture. Inadequate water availability due to absorption by BA can inhibit the hydration process [115], thereby increasing the shrinkage rate. This shrinkage can potentially increase porosity and the emergence of microcracks [116], especially in the interface transition zone (ITZ). Understanding these microstructures is essential for evaluating concrete's mechanical properties and durability after long-term immersion. The results of SEM analysis in Fig. 9(b) with a magnification of 2000x identified the microstructure of HVFA-SCC-70 +BA Inner Code concrete at a depth of 1 cm. Portlandite crystals can be seen forming, indicating continuous cement hydration. The C-A-S-H matrix is still dominant but has morphological differences compared to the Outer Code, probably due to differences in internal hydration conditions. The FA particles are more visible with higher magnification, indicating good distribution in the matrix. The difference between the Outer and Inner Code may be due to differences in hydration levels or environmental exposure during immersion.

Figs. 10c and 10(d) show the results of EDS analysis on HVFA-SCC-70 +BA outer code and HVFA-SCC-70 +BA Inner Code samples, which aim to identify the elements in the mixture. After 180 days of immersion, the spectrum shows clear peaks for calcium (Ca), silicon (Si), aluminium (Al), and oxygen (O). The presence of these elements confirms the formation of the primary hydration phase in C-A-S-H, with values of 16.70 %, 7.55 %, 3.08 %, and 52.16 % for the HVFA-SCC-70 +BA Outer Code variation, respectively, as well as 9.51 %, 9.51 %, 4.42 % and 49.55 % for the HVFA-SCC-70 +BA Inner Code variation. EDS analysis also identifies the composition of other elements, including C, N, Na, Mg, P, S, Cl, K, and Fe. More calcium and silica indicate that most of the C-A-S-H gels have formed and developed in the studied SCC mixtures [117–119]. This EDS analysis supports the SEM findings and provides quantitative information about the composition of the elements.

A comparison between SEM and EDS images of the Outer and Inner Code reveals significant differences in the microstructure and composition of the elements. SEM images show that the Outer Code has more microcracks, likely due to direct exposure to the immersion environment. In contrast, the Inner Code shows a more pronounced formation of portlandite crystals, which indicates a continuous hydration process in the concrete. The quantitative differences seen in the EDS spectrum also reveal variations in the composition of the hydration phase. These findings are crucial to understanding the impact of long-term immersion on HVFA-SCC concrete and its implications for durability.

Based on SEM and EDS test data, immersion of HVFA-SCC concrete in the tidal zone for 180 days results in the formation of C-A-S-H and a continuous pozzolanic reaction, increasing the density and durability of the concrete. The variation between the Outer and Inner Code emphasizes the need to pay attention to microstructural differences in durability analysis. This research supports using FA and BA to produce more durable concrete. However, the presence of microcracks suggests that further research is still needed to optimize the concrete mix and minimize potential damage.

### 3.5.2. XRD (Energy dispersive X-ray spectroscopy)

The X-ray diffraction (XRD) pattern displayed in Fig. 11 reveals a complex crystallinity profile between the inner and outer sections of the HVFA-SCC-70 +BA specimen, which has been immersed for 180 days in the tidal zone of seawater. The main peaks at 2θ angles around 22°, 27°, and 28° are dominated by quartz, labradorite, and albite minerals, affirming that the composition of the concrete is rich in FA and BA. The high intensity of the peaks, although indicating a dominant crystalline phase, also suggests that the hydration reaction has not been fully completed. In other words, these minerals have not entirely transformed into amorphous phases, meaning there are still reactants available for further reactions in the subsequent stages.

A significant difference between the inner and outer sections is observed in the intensity of the Calcium Aluminate Silicate Hydrates (CASH) peaks. In the inner section, the CASH peaks are more pronounced and stronger, indicating better formation in that area. Conversely, the CASH peaks in the outer section are considerably weaker, suggesting degradation or inhibition in the formation of this

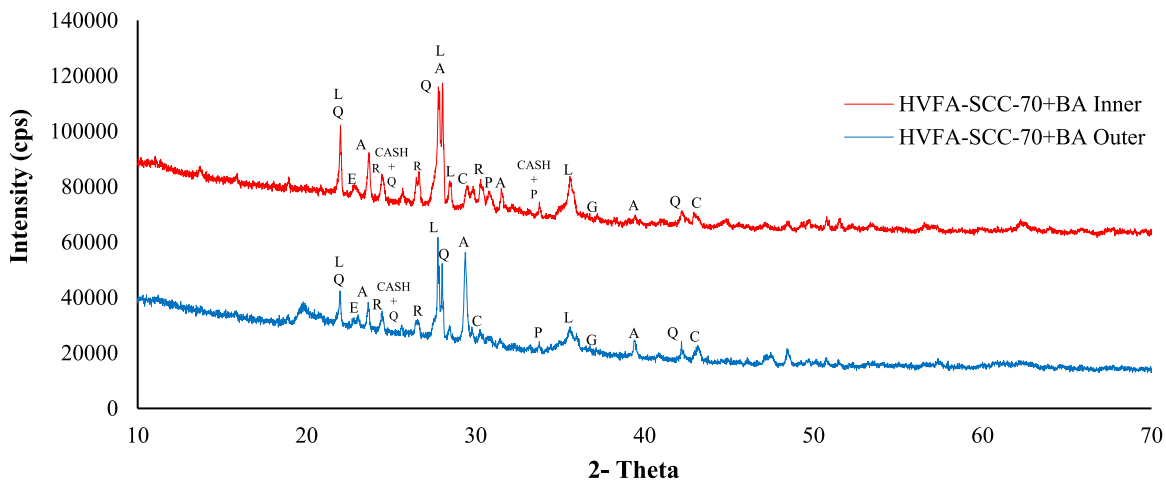


**Fig. 11.** XRD pattern of HVFA-SCC-70 +BA at 180 days (L = Labradorite; Q = Quartz; A = Albite; P = Portlandite, R = Rosenhahnite; E = Ettringite; C = Calcite; G = Gypsum; CASH = Calcium aluminate silicate hydrates).

phase. This phenomenon occurs because the outer section is directly exposed to the aggressive tidal environment, where sulfate, chloride, and carbonate ions from seawater induce changes in the microstructure of the concrete [120].

Portlandite indicates that the hydration process is still ongoing in the HVFA-SCC concrete. Portlandite forms from the hydration of tricalcium silicate (C3S), dicalcium silicate (C2S), tricalcium aluminate (C3A), tetra calcium aluminoferrite (C4AF), and gypsum in the cement when mixed with water [121]. However, a decrease in the intensity of the peak of portlandite in the outer part indicates a transformation due to carbonation [122]. However, the reduction in the intensity of the portlandite peaks in the outer section indicates a transformation due to carbonation [122]. This transformation reduces portlandite's ability to stabilize pH, subsequently leading to the destabilization of Calcium Silicate Hydrate (C-S-H). One of the main factors in this reduction is the carbonation reaction, where portlandite reacts with CO<sub>2</sub> from the air or seawater to form calcite (CaCO<sub>3</sub>). The sulfate attack that generates gypsum can also diminish the portlandite present.

The presence of rosenhahnite, a calcium silicate hydrate mineral, has been detected in the concrete samples, with relatively higher peak intensities in the outer section. This indicates the possibility of ongoing hydration reactions or microstructural transformations due to environmental exposure. The XRD graph also reveals the presence of ettringite and gypsum, reflecting the complex interactions between the initial material composition and environmental conditions. Although sulfate attack from seawater significantly contributes to the formation of both minerals [123], particularly in the outer section. It is important to note that gypsum is added to Portland cement as a setting time regulator [124]. Therefore, the higher peak intensity in the outer section reflects more intense sulfate exposure and the accumulation of initial material sources that are increasingly enriched by reactions with sulfate ions from seawater.

The controlled ettringite formation can fill the pores in concrete, enhancing density and reducing permeability. On the other hand, gypsum plays a crucial role in regulating the early hydration reactions. The interaction between these two minerals and pozzolanic materials in HVFA-SCC concrete can improve long-term durability, especially in aggressive environments, through self-healing mechanisms and the formation of beneficial additional hydration phases such as C-A-S-H.

In the Control-70 specimens, as shown in Fig. 12, the XRD analysis reveals differences in crystallinity profiles between the inner and outer sections after 180 days of immersion. The detected peaks indicate the presence of key crystalline phases such as quartz, ettringite, gypsum, portlandite, C-S-H, and C-A-S-H. The decrease in the intensity of the portlandite peak in the outer section suggests carbonation has occurred, while the broader and less sharp patterns of C-S-H and C-A-S-H indicate variations in the formation processes and transformations of these phases.

The difference in the intensity of the ettringite and gypsum peaks between the inner and outer sections of Control-70 indicates permeability variations. With higher permeability, the outer section is more susceptible to the penetration of sulfate ions from the seawater environment, leading to the increased formation of ettringite and gypsum. This suggests that Control-70 is vulnerable to sulfate attack, particularly on surfaces exposed to these conditions.

The XRD analysis indicates that HVFA-SCC-70 +BA performs better than Control-70 in tidal environments. The formation of more optimal hydration phases, higher resistance to sulfate attack, and the potential for continued reactivity from pozzolanic materials underscore the significant benefits of adding FA and BA. Therefore, HVFA-SCC-70 +BA is recommended as a more suitable concrete variation for applications in tidal environments, with positive implications for the long-term durability of concrete structures.

### 3.6. Durability analysis

#### 3.6.1. Chloride ion concentration

The results of the chloride ion concentration tests on HVFA-SCC concrete during a 240-day immersion period in the tidal zone, as shown in Fig. 13, indicate a significant variation in chloride ion content among the three concrete types assessed, both at depths of

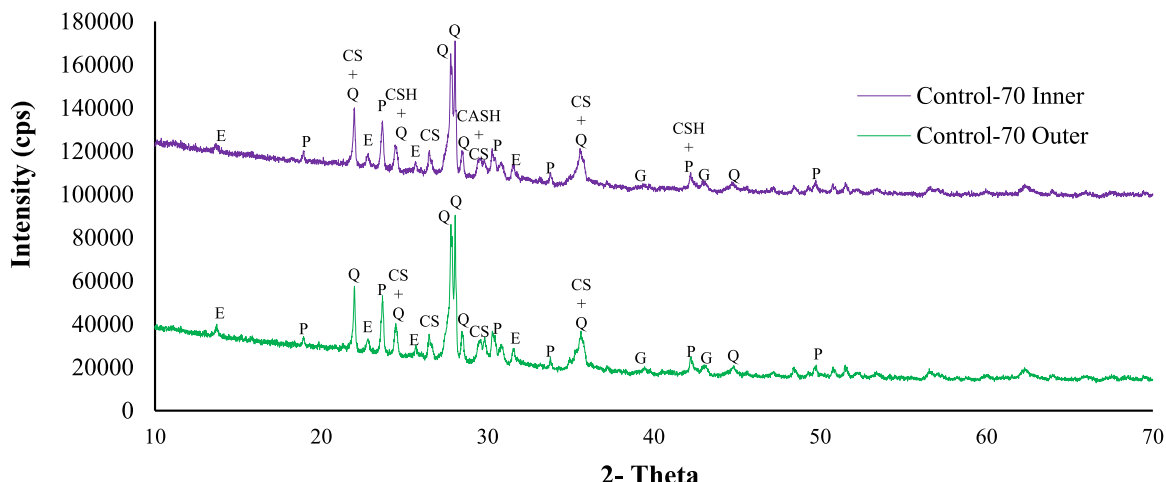


**Fig. 12.** XRD pattern of Control-70 at 180 days (Q = Quartz; P = Portlandite; E = Ettringite; G = Gypsum; CS = Calcium silicates; CASH = Calcium aluminate silicate hydrates).

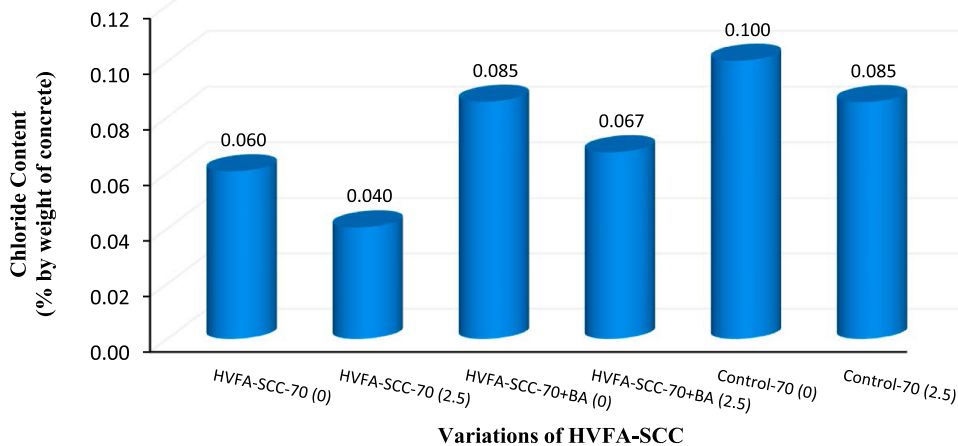


**Fig. 13.** Chloride concentration of HVFA-SCC concrete at depths of 0 cm and 2.5 cm.

0 cm and 2.5 cm. At a depth of 0 cm, the Control-70 concrete exhibited the highest chloride ion content at 0.100 %, followed by HVFA-SCC-70 +BA at 0.085 % and HVFA-SCC-70 at 0.060 %. A similar pattern was observed at a depth of 2.5 cm, albeit with lower values. The chloride ion content in Control-70 remained the highest at 0.085 %, followed by HVFA-SCC-70 +BA at 0.067 % and HVFA-SCC-70 at 0.040 %. The decrease in chloride ion content at this depth suggests that chloride ions tend to concentrate at the surface and diminish as they penetrate deeper into the concrete. Notably, HVFA-SCC-70 demonstrated the best resistance to chloride ion penetration compared to the other variations. It is important to highlight that all three mixtures maintained chloride concentrations below the maximum threshold for corrosion risk, which is set at 0.14 % and is regarded as a high chloride concentration [125]. Several factors influence the chloride threshold levels [126], [127], including the type of chloride salt [128], supplementary cementitious materials in cement-based mixtures [129], and the source of chloride [130].

The incorporation of FA in HVFA-SCC significantly benefits the reduction of chloride ion penetration. Concrete mixtures containing FA exhibit a more compact microstructure, leading to lower permeability and decreased diffusion of chloride ions, ultimately enhancing the durability of the concrete (Argiz et al., 2017; Liu et al., 2013; Menéndez et al., 2019). The addition of BA in HVFA-SCC-70 +BA also yields positive effects, albeit not as pronounced as in HVFA-SCC-70. While BA can reduce chloride ion penetration, it is less effective than FA in improving the concrete's resistance to aggressive environments. The complex interactions between the characteristics of the constituent materials and the hydration process influence the chloride content in SCC mixtures containing HVFA and BA. BA particles' porous nature and irregular shape can affect water distribution during hydration [109], [128], which, in turn, impacts shrinkage and the formation of voids within the concrete matrix. Uncontrolled shrinkage may contribute to the development of micro-cracks [116], particularly in the interfacial transition zone (ITZ), potentially affecting chloride ion penetration [134,135]. This analysis underscores the significance of ash content in the mixtures, as it significantly influences concrete performance against corrosion [131].

The Control-70 concrete, which does not incorporate supplementary materials, exhibits vulnerabilities when exposed to tidal environments. The high chloride ion content at the surface and depth indicates that this concrete is more susceptible to aggressive environments rich in chloride ions [34], [46]. This susceptibility may accelerate the corrosion of the reinforcing steel within the concrete, thereby diminishing the structure's service life.

In contrast, the combination of HVFA, BA, NaOH, and CaCO<sub>3</sub> demonstrates an enhanced durability of SCC in tidal zones after 240 days of immersion. Although the chloride ion concentration is slightly higher than in the mixtures without BA, the results remain within safe limits. HVFA has been shown to reduce porosity effectively and increase chloride binding capacity, which is crucial for preventing corrosion in marine environments [136,137]. As a replacement for natural fine aggregate (NFA), BA positively contributes to the durability and mechanical properties of HVFA-SCC, reducing chloride permeability and enhancing the concrete's resistance to chloride attack over time [138]. Moreover, NaOH can enhance the pozzolanic reactions of FA and BA, resulting in additional calcium silicate hydrate (C-S-H) gel that strengthens the microstructure and the overall strength of the concrete [139]. The incorporation of CaCO<sub>3</sub> can further reduce porosity by filling voids and enhancing nucleation effects, thereby improving the concrete's resistance to chloride migration [67,68].

This study reinforces the findings of Menéndez et al. [131]. The test results indicate that the chloride diffusion coefficient significantly decreases from  $23 \times 10^{-12}$  m<sup>2</sup>/s in concrete without coal ash to  $4.5 \times 10^{-12}$  m<sup>2</sup>/s in concrete containing 35 % coal ash (by weight of cement). This reduction reflects an enhanced resistance of the concrete to chloride ion penetration. These findings are consistent with Zaimi et al. [140], who stated that concrete containing BA exhibits superior chloride resistance. Thus, using BA can enhance the concrete's resilience against chloride penetration.

On the other hand, Moffatt et al. [34] conducted chloride ion penetration tests on HVFA concrete. They discovered that the chloride penetration depth in concrete without FA exceeded 100 mm. In contrast, in concrete containing FA, the penetration depth was reduced

to approximately 30–40 mm. Therefore, it can be concluded that FA-containing concrete demonstrates greater resistance to chloride ion penetration over the long term. However, differing results presented by Syah et al. [137] Although HVFA can reduce chloride penetration due to its pozzolanic properties and improved pore structure, adding BA may increase the level of chloride penetration. This is attributed to BA's higher porosity, which facilitates chloride ingress.

From the analysis, it can be concluded that concrete without BA shows slightly better chloride resistance. However, the use of BA is still recommended due to its additional benefits and compliance with quality standards. To optimize the use of BA, further research is needed to mitigate the shrinkage effects that can lead to cracking and ensure that resistance to chloride penetration remains optimal. Strategies such as using appropriate curing compounds, adding fibers, and optimizing BA proportions should be explored in greater depth to prevent shrinkage-induced cracking and reduce the risk of chloride penetration. Additionally, careful mixture design and strict quality control measures are essential to maximize the benefits of BA.

### 3.6.2. Sulfate ion concentration

**Fig. 14** presents the results of sulfate concentration testing in HVFA-SCC concrete after exposure to the tidal zone for 240 days. The analysis reveals that the HVFA-SCC-70 variation exhibits the lowest sulfate levels compared to other variations, specifically 4.828 % at a depth of 0 cm and 3.608 % at a depth of 2.5 cm. This low sulfate concentration indicates the effectiveness of fly ash (FA) as a cement substitute in enhancing the concrete's resistance to sulfate attack. FA, with its pozzolanic properties, interacts with calcium hydroxide  $\text{Ca}(\text{OH})_2$  produced from cement hydration, forming a denser and less permeable calcium silicate hydrate (C-S-H) [141]. This denser microstructure contributes to improved strength and durability of the concrete [96], [97], thereby inhibiting the penetration of sulfate ions into the concrete matrix [132], [133]. These findings align with Menéndez et al. [140], who state that increased FA content correlates with enhanced resistance to sulfate attacks. The utilization of a minimum of 25 % FA has proven to provide a significant improvement in resistance to sulfate exposure.

Adding BA to HVFA-SCC-70 concrete results in an increased sulfate concentration compared to mixtures utilizing only FA, with levels reaching 5.323 % at a depth of 0 cm and 4.458 % at a depth of 2.5 cm. This phenomenon can be attributed to BA and FA's differing physical and chemical properties. BA features larger particle sizes and irregular shapes, contributing to lower reactivity and higher water absorption capacity. The larger pores in BA allow for greater water absorption, which may lead to increased sulfate levels, as the entrapped water could contain dissolved sulfates that react with the concrete matrix [142]. Despite BA's lower reactivity than FA, its inclusion in HVFA-SCC mixtures can still enhance the concrete's resistance to sulfate attack. It is important to note that although sulfate levels in BA-containing concrete are higher, they remain below the threshold of 5.5 % [143], indicating that the overall performance is still acceptable.

Integrating BA in construction materials, particularly for enhancing sulfate resistance, can be optimized by adding additives such as NaOH and  $\text{CaCO}_3$ . These additives play a crucial role in improving the density and reducing the porosity of the BA matrix, thereby strengthening the material's resistance to sulfate attack. The presence of  $\text{CaCO}_3$  contributes to the formation of calcium silicate hydrate, which is essential for enhancing the strength and durability of concrete by decreasing porosity and improving the mechanical properties of the concrete matrix [144]. Meanwhile, NaOH is known to effectively activate pozzolanic materials, increasing the solubility and reactivity of silicates to form a dense gel. This results in a less porous matrix with improved resistance to chemical attacks [145]. The combination of NaOH and  $\text{CaCO}_3$  has the potential to enhance the packing density and chemical stability of HVFA-SCC mixtures, significantly contributing to improved sulfate resistance.

Control-70, which contains neither FA nor BA, exhibits the highest sulfate concentration among all variations, reaching 6.612 % at a depth of 0 cm and 5.330 % at a depth of 2.5 cm. This data indicates that the sulfate attack levels on the concrete surface are significantly elevated, surpassing the established threshold. This phenomenon underscores the importance of incorporating pozzolanic additives such as FA and BA to enhance concrete's resistance to sulfate attack, particularly in tidal environments. The high sulfate levels in the control concrete highlight the necessity for modifying concrete mixtures to improve durability under extreme environmental conditions. These findings suggest that HVFA concrete can deliver comparable, if not superior, performance and durability compared to traditional concrete, especially in marine applications [95].

To optimize the potential of BA, particularly in coastal infrastructure vulnerable to chemical attacks, in-depth research is required to determine the ideal proportion of BA by integrating analyses of porosity and shrinkage factors in HVFA-SCC concrete, design mixtures that enhance sulfate resistance and minimize the risk of cracking due to hydration shrinkage. Furthermore, innovative exploration into the use of chemical additives such as NaOH and  $\text{CaCO}_3$  can address the inherent weaknesses of BA, creating strong, durable, and environmentally friendly materials. This approach will pave the way for more efficient and sustainable construction solutions amid increasingly challenging environmental conditions.

## 4. Conclusions

This paper presents an experimental study on the mechanical properties, microstructure, and durability of High Volume Fly Ash - Self Compacting Concrete (HVFA-SCC) after exposure to tidal zones for 240 days. The main conclusions of the research are as follows:

Substituting 20 % bottom ash for sand reduces the workability of HVFA-SCC. However, incorporating 0.05 Molar NaOH and 5 %  $\text{CaCO}_3$  effectively enhances workability to meet SCC requirements.

All HVFA-SCC variations showed a significant flexural capacity increase of 10.78–30.49 % from 30 day to 240 days. In contrast, Control-60 and Control-70 declined by 15.44 % and 14.36 %, respectively, between 60 and 240 days.

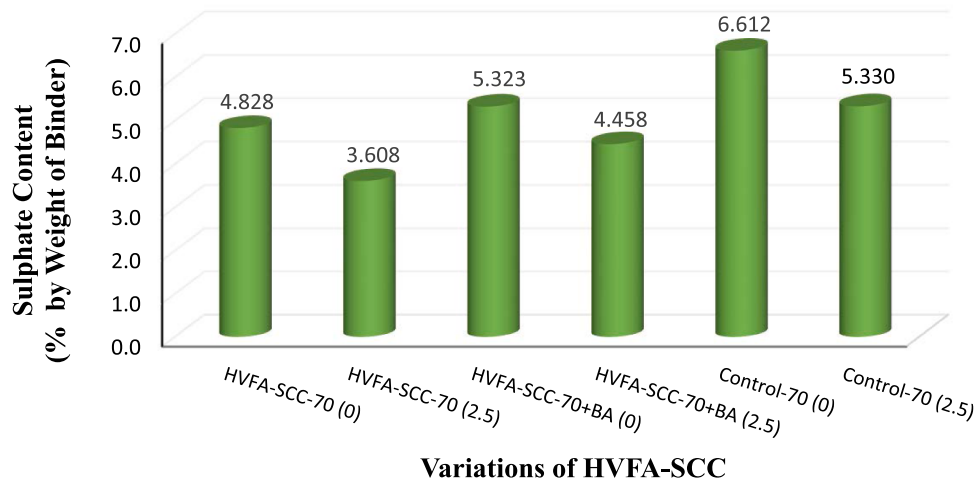


**Fig. 14.** Sulfate concentration of HVFA-SCC concrete at depths of 0 cm and 2.5 cm.

HVFA-SCC-60 and HVFA-SCC-70 achieved optimal compressive strengths of 64.12 MPa and 59.44 MPa, respectively, at 240 days of immersion under tidal conditions, both exceeding the control concrete's strength

HVFA-SCC-70 +BA demonstrates significant superiority over Control-70 in sulfate resistance (XRD), supported by enhanced C-A-S-H formation (SEM/EDS), despite the appearance of microcracks due to environmental conditions and shrinkage.

HVFA-SCC-70 shows the best resistance to chloride and sulfate ion penetration in the tidal zone, while Control-70 is more susceptible to corrosion

The combination of HVFA, BA, NaOH, and CaCO<sub>3</sub> (HVFA-SCC-70 +BA) effectively enhances the durability of concrete in tidal environments, with chloride and sulfate concentrations below threshold levels.

Developing HVFA-SCC concrete with bottom ash requires in-depth research to address cracking due to excessive water absorption through proportion optimization, innovative additives, and appropriate bottom ash processing methods.

#### Declaration of Competing Interest

The authors declare the following financial interests/personal relationships which may be considered as potential competing interests: Januarti Jaya Ekaputri reports financial support was provided by National Research and Innovation Agency, Indonesia by the contract number 6/IV/KS/05/2023 and 1179/PKS/ITS/2023 for support this research. Januarti Jaya Ekaputri reports a relationship with Sepuluh Nopember Institute of Technology that includes travel reimbursement. Januarti Jaya Ekaputri reports equipment, drugs, or supplies were provided by Institut Teknologi Sepuluh Nopember. Juandra Hartono also reports financial support by Lembaga Pengelola Dana Pendidikan (LPDP), Ministry of Finance, Republic of Indonesia for his doctoral study. If there are other authors, they declare that they have no known competing financial interests or personal relationships that could have appeared to influence the work reported in this paper. If there are other authors, they declare that they have no known competing financial interests or personal relationships that could have appeared to influence the work reported in this paper.

#### Acknowledgments

We thank the Lembaga Pengelola Dana Pendidikan (LPDP), Ministry of Finance, Republic of Indonesia, for their support and financial assistance for doctoral scholarship to JH. JJE was supported by National Research and Innovation Agency, Indonesia, with the contract number 6/IV/KS/05/2023 and 1179/PKS/ITS/2023 for support of this research. We also appreciate the Balai Besar Pelaksanaan Jalan Nasional Jawa Timur Bali (BBPJN), Ministry of Public Works and Housing, Indonesia, and PT Varia Usaha Beton, East Java and Central Java Plant, Republic of Indonesia, for their contributions.

#### Data availability

Data will be made available on request.

#### References

- [1] M.J. Osmolska, T. Kanstad, M.A.N. Hendriks, K. Hornbostel, G. Markeset, Durability of pretensioned concrete girders in coastal climate bridges: basis for better maintenance and future design, Struct. Concr. 20 (6) (Dec. 2019) 2256–2271, <https://doi.org/10.1002/suco.201900144>.
- [2] H. Zhou, et al., Field test of a reinforced concrete bridge under marine environmental corrosion, Eng. Fail Anal. 115 (Sep. 2020), <https://doi.org/10.1016/j.engfailanal.2020.104669>.

- [3] V. Herry, R.P. Sastrawiria, H.A. Halim, and Septinurriandiani, *Damage Identification & Bridge Condition Valuation to Support Bridge Asset Management*, 1st ed. Jakarta: Road and Bridge Research and Development Center, Ministry of Public Works and Public Housing, 2017.
- [4] L. Suharinah, "Final Report on Bridge Reinforced Concrete Damage Due to Corrosive Environment," Bandung, 2000.
- [5] J. Haarpaintner, C. Davids, Mapping atmospheric exposure of the intertidal zone with sentinel-1 csar in northern Norway, *Remote Sens.* 13 (17) (Sep. 2021), <https://doi.org/10.3390/rs13173354>.
- [6] C. Chen, C. Zhang, B. Tian, W. Wu, Y. Zhou, Tide2Topo: A new method for mapping intertidal topography accurately in complex estuaries and bays with time-series Sentinel-2 images, *ISPRS J. Photogramm. Remote Sens.* 200 (Jun. 2023) 55–72, <https://doi.org/10.1016/j.isprsjprs.2023.05.004>.
- [7] P.S. Petraitis, J.A.D. Fisher, S. Dudgeon, *Rocky Intertidal Zone*, Elsevier B.V, 2008, pp. 3107–3113.
- [8] S. Vogel, *Comparative Biomechanics*, in *Life's Physical World*, Princeton University Press, New Jersey, 2013.
- [9] V. Perricone, M. Mutalipassi, A. Mele, M. Buono, D. Vicinanza, P. Contestabile, Nature-based and bioinspired solutions for coastal protection: An overview among key ecosystems and a promising pathway for new functional and sustainable designs, Jul. 01, Oxford University Press, 2023, <https://doi.org/10.1093/icesjms/fsad080>.
- [10] J.L. Rodrigues-Filho et al., "From ecological functions to ecosystem services: linking coastal lagoons biodiversity with human well-being," Jul. 01, 2023, *Springer Science and Business Media Deutschland GmbH*. doi: [10.1007/s10750-023-05171-0](https://doi.org/10.1007/s10750-023-05171-0).
- [11] M.G. Lionetto, R. Caricato, M.E. Giordano, Pollution biomarkers in the framework of marine biodiversity conservation: State of art and perspectives, *Water* 13 (13) (Jul. 2021), <https://doi.org/10.3390/w13131847>.
- [12] C. Little, J.A. Kitching, *The Biology of Rocky Shores*, Oxford University Press, 1996.
- [13] C.D.G. Harley, et al., The impacts of climate change in coastal marine systems, *Ecol. Lett.* 9 (2) (Feb. 2006) 228–241, <https://doi.org/10.1111/j.1461-0248.2005.00871.x>.
- [14] G. Leurs, B.O. Nieuwenhuis, T.J. Zuidewind, N. Hijner, H. Olff, L.L. Govers, Where land meets sea: Intertidal areas as key-habitats for sharks and rays, *Fish Fish.* 24 (3) (May 2023) 407–426, <https://doi.org/10.1111/faf.12735>.
- [15] N.J. Murray, et al., High-resolution global maps of tidal flat ecosystems from 1984 to 2019, *Sci. Data* 9 (1) (Dec. 2022), <https://doi.org/10.1038/s41597-022-01635-5>.
- [16] ASTM Standard D1141–98, "Practice for the Preparation of Substitute Ocean Water," Jul. 01, 2021, ASTM International, West Conshohocken, PA. doi: [10.1520/D1141-98R21](https://doi.org/10.1520/D1141-98R21).
- [17] ASTM Standard C1202-12, "Test Method for Electrical Indication of Concretes Ability to Resist Chloride Ion Penetration," West Conshohocken, PA, Feb. 2012. doi: [10.1520/C1202-12](https://doi.org/10.1520/C1202-12).
- [18] ASTM Standard C642 – 13, "Test Method for Density, Absorption, and Voids in Hardened Concrete," West Conshohocken, PA, Feb. 2013. doi: [10.1520/C0642-13](https://doi.org/10.1520/C0642-13).
- [19] ASTM Standard C1012/C1012M – 12, "Test Method for Length Change of Hydraulic-Cement Mortars Exposed to a Sulfate Solution," West Conshohocken, PA, Apr. 2012. doi: [10.1520/C1012\\_C1012M-12](https://doi.org/10.1520/C1012_C1012M-12).
- [20] D.A. Koleva, J.H.W. de Wit, K. van Breugel, Z.F. Lodhi, E. van Westing, Investigation of corrosion and cathodic protection in reinforced concrete, *J. Electrochem. Soc.* 154 (4) (2007) P52, <https://doi.org/10.1149/1.2436609>.
- [21] S.J. Pantazopoulou, J.F. Bonacci, S. Sheikh, A. Thomas, N. Hearn, Repair of corrosion-damaged columns with FRP wraps, *J. Compos. Constr.* (2001) 3.
- [22] K. Kobayashi, T. Iizuka, H. Kurachi, K. Rokugo, Corrosion protection performance of high performance fiber reinforced cement composites as a repair material, *Cem. Concr. Compos.* 32 (6) (Jul. 2010) 411–420, <https://doi.org/10.1016/j.cemconcomp.2010.03.005>.
- [23] S. Masoud, Khaled Soudki, T. Topper, Postrepair fatigue performance of FRP-repaired corroded RC beams: experimental and analytical investigation, *J. Compos. Constr.* 9 (2005), <https://doi.org/10.1061/ASCE1090-02682005:5441>.
- [24] L. Basheer, D.J. Cleland, A.E. Long, Protection provided by surface treatments against chloride induced corrosion, *Mater. Struct.* 31 (1998) 459–464.
- [25] A. Goyal, H.S. Pouya, E. Ganjian, P. Claisse, A review of corrosion and protection of steel in concrete, *Arab J. Sci. Eng.* 43 (10) (Oct. 2018) 5035–5055, <https://doi.org/10.1007/s13369-018-3303-2>.
- [26] V. Kumar, R. Singh, M.A. Quraishi, A study on corrosion of reinforcement in concrete and effect of inhibitor on service life of RCC, *J. Mater. Environ. Sci.* 4 (5) (2013) 726–731.
- [27] C. Jaturapitakkul, K. Kiattikomol, V. Sata, T. Leekeeratikul, Use of ground coarse fly ash as a replacement of condensed silica fume in producing high-strength concrete, *Cem. Concr. Res.* 34 (4) (Apr. 2004) 549–555, [https://doi.org/10.1016/S0008-8846\(03\)00150-9](https://doi.org/10.1016/S0008-8846(03)00150-9).
- [28] K. Kiattikomol, C. Jaturapitakkul, S. Songpiriyakij, S. Chutubtim, A study of ground coarse fly ashes with different finenesses from various sources as pozzolanic materials, *Cem. Concr. Compos.* (2001) 335–343. ([www.elsevier.com/locate/cemconcomp](http://www.elsevier.com/locate/cemconcomp)) ([Online]. Available).
- [29] C. Ozyildirim, "Laboratory Investigation of Nanomaterials to Improve the Permeability and Strength of Concrete," 2010. [Online]. Available: [http://www.virginiadiot.org/vtrc/main/online\\_reports/pdf/r18-r18.pdf](http://www.virginiadiot.org/vtrc/main/online_reports/pdf/r18-r18.pdf).
- [30] M.H. Wolfe, "Bond Strength of High-volume Fly Ash Concrete," Missouri University of Science and Technology, 2011.
- [31] A.S. Budi, E. Safitri, S. Sangadjie, S.A. Kristiawan, Shear Strength of HVFA-SCC Beams without Stirrups, *Buildings* 11 (4) (Apr. 2021) 177, <https://doi.org/10.3390/buildings11040177>.
- [32] M. Li, A review on early age and long-term compressive strength of highvolume flyash concrete (EDP Sciences), *MATEC Web Conf.* (Sep. 2018), <https://doi.org/10.1051/matecconf/201820701004>.
- [33] L.K. Crouch, R. Hewitt, and B. Byard, High Volume Fly Ash Concrete, in 2007 World of Coal Ash (WOCA), Northern Kentucky, USA, 2007, pp. 1–14.
- [34] E.G. Moffatt, M.D.A. Thomas, A. Fahim, Performance of high-volume fly ash concrete in marine environment, *Cem. Concr. Res.* 102 (Dec. 2017) 127–135, <https://doi.org/10.1016/j.cemconres.2017.09.008>.
- [35] C. Herath, C. Gunasekara, D.W. Law, S. Setunge, Performance of high volume fly ash concrete incorporating additives: a systematic literature review, *Constr. Build. Mater.* 258 (Oct. 2020) 120606, <https://doi.org/10.1016/j.conbuildmat.2020.120606>.
- [36] N. Liu et al., Road life-cycle carbon dioxide emissions and emission reduction technologies: A review," Aug. 01, 2022, Chang'an University. doi: [10.1016/j.jctte.2022.06.001](https://doi.org/10.1016/j.jctte.2022.06.001).
- [37] Ministry of Environment and Forestry, "Greenhouse Gas (GHG) Inventory Report and Monitoring, Reporting, Verification (MPV)," Jakarta, Feb. 2020.
- [38] H. Okamura, M. Ouchi, Self-Compacting Concrete, *J. Adv. Concr. Technol.* 1 (1) (Mar. 2003) 5–15.
- [39] J. Liu, S. Zang, F. Yang, R. Hai, Y. Yan, Fracture properties of steel fibre reinforced high-volume fly ash self-compacting concrete, *Case Stud. Constr. Mater.* 18 (Jul. 2023) e02110, <https://doi.org/10.1016/j.jcscm.2023.e02110>.
- [40] C.I. Goodier, *Development of self-compacting concrete*, *Struct. Build.* (2003) 405–414.
- [41] M. Solikin, T. Mulyanto, Mechanical properties of self-compacting concrete incorporated with high volume fly ash, *IOP Conf. Ser. Mater. Sci. Eng.* 821 (1) (Apr. 2020) 012019, <https://doi.org/10.1088/1757-899X/821/1/012019>.
- [42] S.P. Shah, G.R. Lomboy, Future research needs in self-consolidating concrete, *J. Sustain. Cem. Based Mater.* 4 (3–4) (Oct. 2015) 154–163, <https://doi.org/10.1080/21650373.2014.956238>.
- [43] L.-H. Han, G.-H. Yao, Experimental behaviour of thin-walled hollow structural steel (HSS) columns filled with self-consolidating concrete (SCC), *Thin-Walled Struct.* 42 (9) (Sep. 2004) 1357–1377, <https://doi.org/10.1016/j.tws.2004.03.016>.
- [44] P.R. de Matos, R. Junckes, E. Graeff, L.R. Prudêncio, Effectiveness of fly ash in reducing the hydration heat release of mass concrete, *J. Build. Eng.* 28 (Mar. 2020), <https://doi.org/10.1016/j.jobe.2019.101063>.
- [45] N. Bouzoubaa, M. Lachemi, Self-compacting concrete incorporating high volumes of class F fly ash Preliminary results, *Cem. Concr. Res.* (2000) 413–420.
- [46] P. Dinakar, K.G. Babu, M. Santhanam, Durability properties of high volume fly ash self compacting concretes, *Cem. Concr. Compos.* 30 (10) (Nov. 2008) 880–886, <https://doi.org/10.1016/j.cemconcomp.2008.06.011>.
- [47] Y.-S. Choi, J.-G. Kim, K.-M. Lee, Corrosion behavior of steel bar embedded in fly ash concrete, *Corros. Sci.* 48 (7) (Jul. 2006) 1733–1745, <https://doi.org/10.1016/j.corsci.2005.05.019>.

- [48] A.F. Hashmi, M. Shariq, A. Baqi, Use of HVFA concrete for sustainable development: a comprehensive review on mechanical and structural properties, *Arab J. Sci. Eng.* 47 (10) (Oct. 2022) 12265–12288, <https://doi.org/10.1007/s13369-022-06884-5>.
- [49] R.H. Faraj, A.F.H. Sherwani, L.H. Jafer, D.F. Ibrahim, Rheological behavior and fresh properties of self-compacting high strength concrete containing recycled PP particles with fly ash and silica fume blended, *J. Build. Eng.* 34 (Feb. 2021) 101667, <https://doi.org/10.1016/j.jobe.2020.101667>.
- [50] J.H. Filho, M.H.F. Medeiros, E. Pereira, P. Helene, M. Asce, and G.C. Isaia, High-Volume Fly Ash Concrete with and without Hydrated Lime: Chloride Diffusion Coefficient from Accelerated Test, 2013.
- [51] D.F. Velandia, C.J. Lyndale, J.L. Provis, F. Ramirez, Effect of mix design inputs, curing and compressive strength on the durability of Na<sub>2</sub>SO<sub>4</sub>-activated high volume fly ash concretes, *Cem. Concr. Compos.* 91 (Aug. 2018) 11–20, <https://doi.org/10.1016/j.cemconcomp.2018.03.028>.
- [52] W. Feng, Y. Tang, Y. Zhang, C. Qi, L. Ma, L. Li, Partially fly ash and nano-silica incorporated recycled coarse aggregate based concrete: constitutive model and enhancement mechanism, *J. Mater. Res. Technol.* 17 (Mar. 2022) 192–210, <https://doi.org/10.1016/j.jmrt.2021.12.135>.
- [53] R.P. Ribeiro, L.J. Jaramillo Nieves, A.M. Bernardin, Effect of fiberglass waste and fly ash addition on the mechanical performance of Portland cement paste, *Clean. Mater.* 7 (Mar. 2023), <https://doi.org/10.1016/j.clema.2023.100176>.
- [54] M. Maizuar, H. Fithra, K. Yusuf, N. Usrina, S. Bahri, S.F. Senin, Mechanical properties of high-volume fly ash mortar modified by hybrid carbon nano tube and graphene oxide, *Electron. J. Struct. Eng.* (Dec. 2024) 23–27, <https://doi.org/10.56748/ejse.24659>.
- [55] G.L. Golewski, Assessing of water absorption on concrete composites containing fly ash up to 30% in regards to structures completely immersed in water, *Case Stud. Constr. Mater.* 19 (Dec. 2023), <https://doi.org/10.1016/j.cscm.2023.e02337>.
- [56] G.L. Golewski, Determination of fracture mechanic parameters of concretes based on cement matrix enhanced by fly ash and nano-silica, *Materials* 17 (17) (Sep. 2024), <https://doi.org/10.3390/ma17174230>.
- [57] G.L. Golewski, Using digital image correlation to evaluate fracture toughness and crack propagation in the mode I testing of concretes involving fly ash and synthetic nano-SiO<sub>2</sub>, *Mater. Res. Express* 11 (9) (Sep. 2024), <https://doi.org/10.1088/2053-1591/ad755e>.
- [58] G.L. Golewski, Enhancement fracture behavior of sustainable cementitious composites using synergy between fly ash (FA) and nanosilica (NS) in the assessment based on digital image processing procedure, *Theor. Appl. Fract. Mech.* 131 (Jun. 2024), <https://doi.org/10.1016/j.tafmec.2024.104442>.
- [59] A. Meena, N. Singh, S.P. Singh, High-volume fly ash self consolidating concrete with coal bottom ash and recycled concrete aggregates: fresh, mechanical and microstructural properties, *J. Build. Eng.* 63 (Jan. 2023), <https://doi.org/10.1016/j.jobe.2022.105447>.
- [60] N. Singh, M. M, S. Arya, Utilization of coal bottom ash in recycled concrete aggregates based self compacting concrete blended with metakaolin, *Resour. Conserv Recycl.* 144 (May 2019) 240–251, <https://doi.org/10.1016/j.resconrec.2019.01.044>.
- [61] M. Singh, R. Siddique, Strength properties and micro-structural properties of concrete containing coal bottom ash as partial replacement of fine aggregate, *Constr. Build. Mater.* 50 (2014) 246–256, <https://doi.org/10.1016/j.conbuildmat.2013.09.026>.
- [62] M. Singh, R. Siddique, Effect of coal bottom ash as partial replacement of sand on workability and strength properties of concrete, *J. Clean. Prod.* 112 (Jan. 2016) 620–630, <https://doi.org/10.1016/j.jclepro.2015.08.001>.
- [63] M. Rafieizonooz, J. Mirza, M.R. Salim, M.W. Hussin, E. Khankhaje, Investigation of coal bottom ash and fly ash in concrete as replacement for sand and cement, *Constr. Build. Mater.* 116 (Jul. 2016) 15–24, <https://doi.org/10.1016/j.conbuildmat.2016.04.080>.
- [64] P. Arjunan, M.R. Silsbee, D.M. Roy, Chemical Activation of Low Calcium Fly Ash Part 1: identification of suitable activators and their dosage, *Int. Ash Util. Symp.* (2001).
- [65] A. Fernández-Jiménez, I. García-Lodeiro, and A. Palomo, Alkaline activation-induced conversion of fly ash into an effective binder Part III. Reducing the clinker content, in: Proc. of the EUROCOALASH 2012 Conference, 2012. [Online]. Available: <http://www.evipar.org/>.
- [66] W.D. Pratiwi, Triwulan, J.J. Ekaputri, H. Fansuri, Combination of precipitated-calcium carbonate substitution and dilute-alkali fly ash treatment in a very high-volume fly ash cement paste, *Constr. Build. Mater.* 234 (Feb. 2020), <https://doi.org/10.1016/j.conbuildmat.2019.117273>.
- [67] F.M. Nejad, M. Tolouei, H. Nazari, A. Naderan, Effects of calcium carbonate nanoparticles and fly ash on mechanical and permeability properties of concrete, *Adv. Civ. Eng.* 7 (1) (Nov. 2018) 651–668, <https://doi.org/10.1520/ACEM20180066>.
- [68] F.U.A. Shaikh, S.W.M. Supit, Mechanical and durability properties of high volume fly ash (HVFA) concrete containing calcium carbonate (CaCO<sub>3</sub>) nanoparticles, *Constr. Build. Mater.* 70 (Nov. 2014) 309–321, <https://doi.org/10.1016/j.conbuildmat.2014.07.099>.
- [69] Z. Yang, S. Liu, L. Yu, L. Xu, A comprehensive study on the hardening features and performance of self-compacting concrete with high-volume fly ash and slag, *Materials* 14 (15) (Aug. 2021), <https://doi.org/10.3390/ma14154286>.
- [70] V. Bonavetti, H. Donza, G. Menéndez, O. Cabrera, E.F. Irassar, Limestone filler cement in low w/c concrete: a rational use of energy, *Cem. Concr. Res.* 33 (6) (Jun. 2003) 865–871, [https://doi.org/10.1016/S0008-8846\(02\)01087-6](https://doi.org/10.1016/S0008-8846(02)01087-6).
- [71] J. Péra, S. Husson, B. Guilhot, Influence of finely ground limestone on cement hydration, *Cem. Concr. Compos.* 21 (2) (1999) 99–105, [https://doi.org/10.1016/S0958-9465\(98\)00020-1i](https://doi.org/10.1016/S0958-9465(98)00020-1i).
- [72] F.U.A. Shaikh, S.W.M. Supit, Chloride induced corrosion durability of high volume fly ash concretes containing nano particles, *Constr. Build. Mater.* 99 (Nov. 2015) 208–225, <https://doi.org/10.1016/j.conbuildmat.2015.09.030>.
- [73] S. Kawashima, P. Hou, D.J. Corr, S.P. Shah, Modification of cement-based materials with nanoparticles, *Cem. Concr. Compos.* (Feb. 2013) 8–15, <https://doi.org/10.1016/j.cemconcomp.2012.06.012>.
- [74] EFNARC, The European Guidelines for Self-Compacting Concrete Specification, Production and Use, May 2005.
- [75] Directorate of Road and Bridge Engineering, NSPK for FABA Utilization in Road Infrastructure Works, Jakarta, Oct. 2022.
- [76] ASTM C150/C150M – 19a, Standard Specification for Portland Cement, Dec. 2019. doi: [10.1520/C0150\\_C0150M-19A](https://doi.org/10.1520/C0150_C0150M-19A).
- [77] ASTM Standard C618-19, Standard Specification for Coal Fly Ash and Raw or Calcined Natural Pozzolan for Use in Concrete C618-19, West Conshohocken, PA, May 2019. doi: [10.1520/C0618-19](https://doi.org/10.1520/C0618-19).
- [78] ASTM Standard C 494/C 494M – 05a, Standard Specification for Chemical Admixtures for Concrete, Jan. 2006.
- [79] ACI 211.4R-08, Guide for Selecting Proportions for High-strength Concrete Using Portland Cement and Other Cementitious Materials, American Concrete Institute, 2008.
- [80] ASTM C78/C78M-21, Standard Test Method for Flexural Strength of Concrete (Using Simple Beam with Third-Point Loading) 1, 2021. doi: [10.1520/C0078\\_C0078M-21](https://doi.org/10.1520/C0078_C0078M-21).
- [81] ASTM Standard C39/C39M-18, Standard Test Method for Compressive Strength of Cylindrical Concrete Specimens, 2018. doi: [10.1520/C0039\\_C0039M-18](https://doi.org/10.1520/C0039_C0039M-18).
- [82] ASTM Standard C1556-04, Standard Test Method for Determining the Apparent Chloride Diffusion Coefficient of Cementitious Mixtures by Bulk Diffusion, 2004. [Online]. Available: [www.astm.org](http://www.astm.org).
- [83] ASTM Standard C114-09, Standard Test Methods for Chemical Analysis of Hydraulic Cement, 2009. [Online]. Available: [www.astm.org](http://www.astm.org).
- [84] G. Baert, A.M. Poppe, N.D. Belie, Strength and durability of high volume flyash concrete, *Struct. Concr.* 9 (2) (Jun. 2008) 101–108, <https://doi.org/10.1680/stco.2008.9.2.101>.
- [85] E. Sakai, S. Miyahara, S. Ohsawa, S.H. Lee, M. Daimon, Hydration of fly ash cement, *Cem. Concr. Res.* 35 (6) (Jun. 2005) 1135–1140, <https://doi.org/10.1016/j.cemconres.2004.09.008>.
- [86] J. Tangpaganit, R. Cheerarat, C. Jaturapitakkul, K. Kiattikomol, Packing effect and pozzolanic reaction of fly ash in mortar, *Cem. Concr. Res.* 35 (6) (Jun. 2005) 1145–1151, <https://doi.org/10.1016/j.cemconres.2004.09.030>.
- [87] A.A. Kadir, M.I.H. Hassan, M.M.A.B. Abdullah, Investigation on Leaching Behaviour of Fly Ash and Bottom Ash Replacement in Self-Compacting Concrete. IOP Conference Series: Materials Science and Engineering, Institute of Physics Publishing, 2016, [10.1088/1757-899X/133/1/012036](https://doi.org/10.1088/1757-899X/133/1/012036).
- [88] N. Ankur, N. Singh, Performance of cement mortars and concretes containing coal bottom ash: A comprehensive review, Elsevier Ltd, Oct. 01, 2021, <https://doi.org/10.1016/j.rser.2021.111361>.
- [89] H. Boutkhlil, et al., Strength characteristics and rheological behavior of a high level of fly ash in the production of concrete, *ACS Omega* 9 (12) (Mar. 2024) 14419–14428, <https://doi.org/10.1021/acsomega.4c00147>.

- [90] T. Xie, T. Ozbakkaloglu, Influence of coal ash properties on compressive behaviour of FA- and BA-based GPC, *Mag. Concr. Res.* 67 (24) (Dec. 2015) 1301–1314, <https://doi.org/10.1680/macr.14.00429>.
- [91] J. Wu, H. Liao, Z. Ma, H. Song, F. Cheng, Effect of different initial CaO/SiO<sub>2</sub> molar ratios and curing times on the preparation and formation mechanism of calcium silicate hydrate, *Materials* 16 (2) (Jan. 2023) 717, <https://doi.org/10.3390/ma16020717>.
- [92] F. Puertas, M. Palacios, H. Manzano, J.S. Dolado, A. Rico, J. Rodriguez, C-A-S-H gels formed in alkali-activated slag cement pastes. Structure and effect on cement properties and durability, *MATEC Web Conf.* 11 (Apr. 2014) 01002, <https://doi.org/10.1051/matecconf/20141101002>.
- [93] S.W.M. Supit, F.U.A. Shaikh, Durability properties of high volume fly ash concrete containing nano-silica, *Mater. Struct.* 48 (8) (Aug. 2015) 2431–2445, <https://doi.org/10.1617/s11527-014-0329-0>.
- [94] Y. Muthusami, K. Phani Soumika, N.Sivakumar Pandiyarajan, B. Mahalingam, Influence of fly ash on rheological behaviour of HVFA concrete, *MATEC Web Conf.* 400 (Jul. 2024) 01001, <https://doi.org/10.1051/matecconf/202440001001>.
- [95] N. Bouzoubaâ, M.H. Zhang, V.M. Malhotra, Mechanical properties and durability of concrete made with high-volume fly ash blended cements using a coarse fly ash, *Cem. Concr. Res.* 31 (10) (Oct. 2001) 1393–1402, [https://doi.org/10.1016/S0008-8846\(01\)00592-0](https://doi.org/10.1016/S0008-8846(01)00592-0).
- [96] M. Raheel, et al., Experimental investigation of quaternary blended sustainable concrete along with mix design optimization, *Structures* 54 (Aug. 2023) 499–514, <https://doi.org/10.1016/j.istruc.2023.05.033>.
- [97] S. Zhang, B. Chen, B. Tian, X. Lu, B. Xiong, Effect of fly ash content on the microstructure and strength of concrete under freeze-thaw condition, *Buildings* 12 (12) (Dec. 2022), <https://doi.org/10.3390/buildings12122113>.
- [98] J. Wang, D. Niu, R. Ma, Y. Zhang, Investigation of sulfate attack resistance of shotcrete under dry-wet cycles, *J. Wuhan. Univ. Technol. Mater. Sci. Ed.* 31 (6) (Dec. 2016) 1329–1335, <https://doi.org/10.1007/s11595-016-1535-0>.
- [99] F. Chen, J. Gao, B. Qi, D. Shen, L. Li, Degradation progress of concrete subject to combined sulfate-chloride attack under drying-wetting cycles and flexural loading, *Constr. Build. Mater.* 151 (Oct. 2017) 164–171, <https://doi.org/10.1016/j.conbuildmat.2017.06.074>.
- [100] C. Phetchuay, S. Horpibulsuk, A. Arulrajah, C. Suksiripattanapong, A. Udomchai, Strength development in soft marine clay stabilized by fly ash and calcium carbide residue based geopolymers, *Appl. Clay Sci.* 127–128 (Jul. 2016) 134–142, <https://doi.org/10.1016/j.clay.2016.04.005>.
- [101] T. Meng, Y. Qiang, A. Hu, C. Xu, L. Lin, Effect of compound nano-CaCO<sub>3</sub> addition on strength development and microstructure of cement-stabilized soil in the marine environment, *Constr. Build. Mater.* 151 (Oct. 2017) 775–781, <https://doi.org/10.1016/j.conbuildmat.2017.06.016>.
- [102] C. Jin, et al., Mechanical properties of high-volume fly ash strain hardening cementitious composite (HVFA-SHCC) for structural application, *Materials* 12 (16) (Aug. 2019), <https://doi.org/10.3390/ma12162607>.
- [103] M. Fajrul Falah, S. Adi Kristiawan, H. Alfisa Saifullah, Tension-stiffening of reinforced HVFA-SCC beams, *Jordan J. Civ. Eng.* 17 (3) (Jul. 2023) 497–512, <https://doi.org/10.14525/JJCE.v17i3.11>.
- [104] I. Wilińska, Investigation of physicochemical processes taking place in chemically activated very high volume fly ash mixtures, *Constr. Build. Mater.* 406 (Nov. 2023), <https://doi.org/10.1016/j.conbuildmat.2023.133359>.
- [105] J. He, C. Sun, X. Wang, Study on the effect of fly ash on mechanical properties and seawater freeze-thaw resistance of seawater sea sand concrete, *Buildings* 14 (7) (Jul. 2024), <https://doi.org/10.3390/buildings14072191>.
- [106] T.C. Madhavi, L.S. Raju, D. Mathur, Durability of strength properties of high volume fly ash concrete, *J. Civ. Eng. Res.* 4 (2014) 7–11.
- [107] G.L. Golewski, Examination of water absorption of low volume fly ash concrete (LVFAC) under water immersion conditions, *Mater. Res Express* 10 (8) (Aug. 2023), <https://doi.org/10.1088/2053-1591/acecf>.
- [108] J.J. Ekaputri, Y. Nurrikizi, The effect of bottom ash on the compressive strength and tensile strength of HVFA concrete, *J. Adv. Civ. Environ. Eng.* 6 (1) (May 2023) 12, <https://doi.org/10.30659/jacee.6.1.12-23>.
- [109] E. Haustein, A. Kurylowicz-Cudowska, Effect of particle size of fly ash microspheres (FAMs) on the selected properties of concrete, *Minerals* 12 (7) (Jul. 2022), <https://doi.org/10.3390/min12070847>.
- [110] A.M. Onaizi and W. Tang, Comparative assessment of the effects of furnace bottom ash and fly ash on mortar performance,” in E3S Web of Conferences, EDP Sciences, Jul. 2024. doi: 10.1051/e3sconf/202454601010.
- [111] K.C. Onyelowe, et al., Multi-objective optimization of sustainable concrete containing fly ash based on environmental and mechanical considerations, *Buildings* 12 (7) (Jul. 2022), <https://doi.org/10.3390/buildings12070948>.
- [112] T. Ali, et al., Investigation on mechanical and durability properties of concrete mixed with silica fume as cementitious material and coal bottom ash as fine aggregate replacement material, *Buildings* 12 (1) (Jan. 2022), <https://doi.org/10.3390/buildings12010044>.
- [113] Y. Liu, B. Dong, S. Hong, Y. Wang, Influence mechanisms of CaCO<sub>3</sub>/NaAlO<sub>2</sub> ratios in carbonaluminate cementitious materials, *J. Mater. Res. Technol.* 25 (Jul. 2023) 4700–4719, <https://doi.org/10.1016/j.jmrt.2023.06.250>.
- [114] H. Baloochi, M. Barra, D. Aponte, Long-term comparison between waste paper fly ash and traditional binder as hydraulic road binder exposed to sulfate concentrations, *Materials* 15 (15) (Aug. 2022), <https://doi.org/10.3390/ma15155424>.
- [115] F. Miguel, J. de Brito, R.V. Silva, Durability-related performance of recycled aggregate concrete containing alkali-activated municipal solid waste incinerator bottom ash, *Constr. Build. Mater.* 397 (Sep. 2023) 132415, <https://doi.org/10.1016/j.conbuildmat.2023.132415>.
- [116] P. Markpiban, W. Krudam, R. Sahamitmongkol, Investigation of flow, compressive strength, shrinkage, and tensile properties of mortar with internal curing bottom ash, *Results Mater.* 15 (Sep. 2022), <https://doi.org/10.1016/j.rimma.2022.100296>.
- [117] A. Jain, R. Gupta, S. Chaudhary, Sustainable development of self-compacting concrete by using granite waste and fly ash, *Constr. Build. Mater.* 262 (Nov. 2020), <https://doi.org/10.1016/j.conbuildmat.2020.120516>.
- [118] R. Sharma, R.A. Khan, Sustainable use of copper slag in self compacting concrete containing supplementary cementitious materials, *J. Clean. Prod.* 151 (May 2017) 179–192, <https://doi.org/10.1016/j.jclepro.2017.03.031>.
- [119] G.A. Lyngdoh, H. Li, M. Zaki, N.M.A. Krishnan, S. Das, Elucidating the constitutive relationship of calcium–silicate–hydrate gel using high throughput reactive molecular simulations and machine learning, *Sci. Rep.* 10 (1) (2020) 21336, <https://doi.org/10.1038/s41598-020-78368-1>.
- [120] H. Sun et al., Combined Effects of Sulfate and Chloride Attack on Steel Reinforced Mortar under Drying-Immersion Cycles, 2022, MDPI. doi: 10.3390/buildings12081252.
- [121] K.K.D. Sungkono, I. Satyarno, H. Priyosulistyo, I. Perdana, Corrosion resistance of high calcium fly ash based reinforced geopolymer concrete in marine environment, *Civ. Eng. Archit.* 11 (5) (Sep. 2023) 3175–3189, <https://doi.org/10.13189/cea.2023.110827>.
- [122] M.N. Seifu, A. Bersisa, K.Y. Moon, G.M. Kim, J.S. Cho, S. Park, Exploring reaction and carbonation products of calcium silicate cement, *J. CO<sub>2</sub> Util.* 71 (May 2023), <https://doi.org/10.1016/j.jcou.2023.102471>.
- [123] C. Li, et al., Understanding the sulfate attack of Portland cement-based materials exposed to applied electric fields: mineralogical alteration and migration behavior of ionic species, *Cem. Concr. Compos.* 111 (Aug. 2020), <https://doi.org/10.1016/j.cemconcomp.2020.103630>.
- [124] A.P. Kirchheim, V. Fernández-Altable, P.J.M. Monteiro, D.C.C. Dal Molin, I. Casanova, Analysis of cubic and orthorhombic C3A hydration in presence of gypsum and lime, *J. Mater. Sci.* 44 (8) (Apr. 2009) 2038–2045, <https://doi.org/10.1007/s10853-009-3292-3>.
- [125] J.P. Broomfield. *Steel Corrosion in Concrete: Fundamentals and Civil Engineering Practice*, 2nd Edition, Taylor & Francis, 2007, p. 201.
- [126] E.Q. Segismundo, L.H. Kim, S.M. Jeong, B.S. Lee, A laboratory study on the filtration and clogging of the sand-bottom ash mixture for stormwater infiltration filter media, *Water* 9 (1) (Jan. 2017), <https://doi.org/10.3390/w9010032>.
- [127] S. Hussain, A.Al-Musallam Rasheeduzzafar, A. Al-Gahatni, Factors affecting threshold chloride for reinforcement corrosion in concrete, *Cem. Concr. Res.* 25 (7) (Apr. 1995) 1543–1555.
- [128] L. Jiang, R. Liu, L. Mo, J. Xu, H. Yang, Influence of chloride salt type on critical chloride content of reinforcement corrosion in concrete, *Mag. Concr. Res.* 65 (5) (Mar. 2013) 319–331, <https://doi.org/10.1680/macr.12.00082>.
- [129] J.H. Kim, J.H. Sung, C.S. Jeon, S.H. Lee, H.S. Kim, A study on the properties of recycled aggregate concrete and its production facilities, *Appl. Sci.* 9 (9) (May 2019), <https://doi.org/10.3390/app9091935>.

- [130] J. Xu, L. Jiang, W. Wang, Y. Jiang, Influence of CaCl<sub>2</sub> and NaCl from different sources on chloride threshold value for the corrosion of steel reinforcement in concrete, Constr. Build. Mater. 25 (2) (Feb. 2011) 663–669, <https://doi.org/10.1016/j.conbuildmat.2010.07.023>.
- [131] E. Menéndez, C. Argiz, M.Á. Sanjuán, Chloride induced reinforcement corrosion in mortars containing coal bottom ash and coal fly ash, Materials 12 (12) (Jun. 2019), <https://doi.org/10.3390/ma12121933>.
- [132] C. Argiz, M.Á. Sanjuán, E. Menéndez, Coal bottom ash for portland cement production, Adv. Mater. Sci. Eng. 2017 (2017) 1–7, <https://doi.org/10.1155/2017/6068286>.
- [133] J. Liu, F. Xing, B.Q. Dong, Microscopic mechanism of the diffusivity of concrete chloride ion, Adv. Mater. Res. (2013) 687–692, <https://doi.org/10.4028/www.scientific.net/AMR.773.687>.
- [134] Q. Yang, Y. Wu, P. Zhi, P. Zhu, Effect of micro-cracks on chloride ion diffusion in concrete based on stochastic aggregate approach, Buildings 14 (5) (May 2024), <https://doi.org/10.3390/buildings14051353>.
- [135] N. Singh, A. Bhardwaj, Shehnazdeep, Permeation behaviour of coal bottom ash concretes, J. Solid Waste Technol. Manag. 48 (3) (Aug. 2022) 353–361, <https://doi.org/10.5276/JSWMTM/2022.353>.
- [136] P.K. Mehta, P.J.M. Monteiro, Concrete Microstructure, Properties, and Materials, Microstruct. Prop. Mater. 3 (2006).
- [137] D.F. Syah, et al., Durability of high-volume fly ash concrete incorporating microbes and bottom ash under accelerated chloride attack, Proc. 4th Int. Conf. Green. Civ. Environ. Eng. (GCEE 2023) (Mar. 2024), <https://doi.org/10.1063/5.0204937>.
- [138] P. Kumar, N. Singh, Influence of recycled concrete aggregates and coal bottom ash on various properties of high volume fly ash-self compacting concrete, J. Build. Eng. 32 (Nov. 2020), <https://doi.org/10.1016/j.jobe.2020.101491>.
- [139] T. Phoo-ngernkham, S. Hanjitsuwan, N. Damrongwiriyayanupap, P. Chindaprasirt, Effect of sodium hydroxide and sodium silicate solutions on strengths of alkali activated high calcium fly ash containing Portland cement, KSCE J. Civ. Eng. 21 (6) (Sep. 2017) 2202–2210, <https://doi.org/10.1007/s12205-016-0327-6>.
- [140] M.N.S. Zaimi, et al., Strength and Chloride Penetration Performance of Concrete Using Coal Bottom Ash as Coarse and Fine Aggregate Replacement, IOP Conference Series Earth and Environmental Science, IOP Publishing Ltd, Feb. 2021, <https://doi.org/10.1088/1755-1315/682/1/012067>.
- [141] E. Menéndez, C. Argiz, M.Á. Sanjuán, Coal ash Portland cement mortars sulphate resistance, Civ. Eng. J. (Iran.) 7 (1) (Jan. 2021) 98–106, <https://doi.org/10.28991/cej-2021-03091640>.
- [142] T. Ali, et al., Investigation on mechanical and durability properties of concrete mixed with silica fume as cementitious material and coal bottom ash as fine aggregate replacement material, Buildings 12 (1) (Jan. 2022), <https://doi.org/10.3390/buildings12010044>.
- [143] G.F. Kheder, D.K. Assi, Limiting total internal sulphates in 15–75 MPa concrete in accordance to its mix proportions, Mater. Struct. 43 (1–2) (Jan. 2010) 273–281, <https://doi.org/10.1617/s11527-009-9487-x>.
- [144] S. Kawashima, J.W.T. Seo, D. Corr, M.C. Hersam, S.P. Shah, Dispersion of CaCO<sub>3</sub> nanoparticles by sonication and surfactant treatment for application in fly ash-cement systems, Mater. Struct. Mater. Et. Constr. 47 (6) (2014) 1011–1023, <https://doi.org/10.1617/s11527-013-0110-9>.
- [145] K. Felaous, A. Aziz, M. Achab, M. Fernández-Raga, A. Benzaouak, Optimizing alkaline activation of natural Volcanic Pozzolan for eco-friendly materials production: an investigation of NaOH molarity and Na<sub>2</sub>SiO<sub>3</sub>-to-NaOH ratio, Sustain. (Switz. ) 15 (5) (Mar. 2023), <https://doi.org/10.3390/su15054453>.